Electronic Supplementary Material (ESI) for Catalysis Science & Technology.
This journal is © The Royal Society of Chemistry 2021

## 1. Thermogravimetric analysis

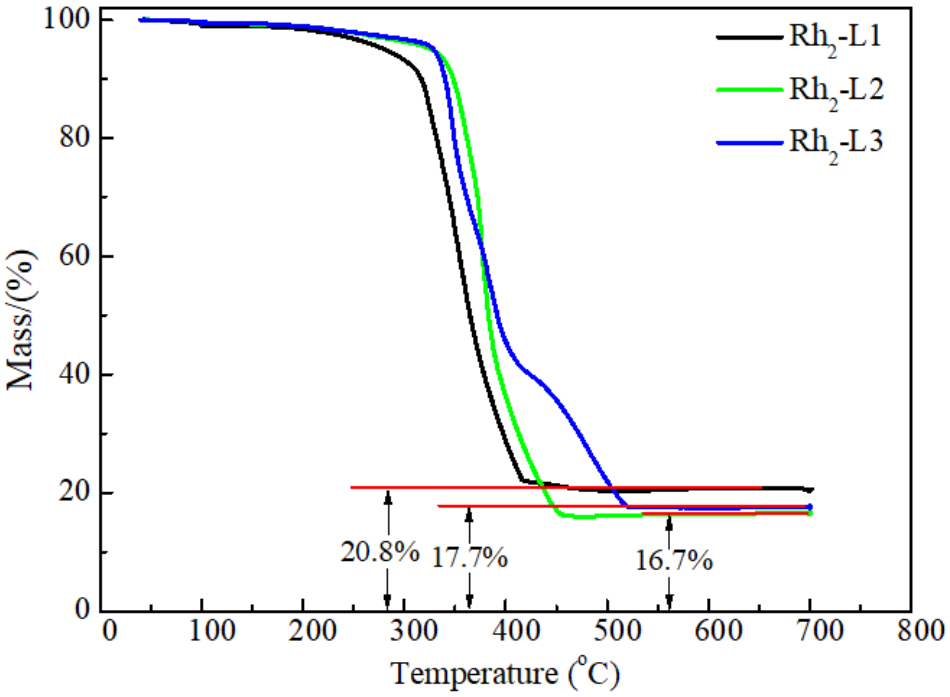


**Figure S1.** TG spectra of $Rh_2$-L1, $Rh_2$-L2 and $Rh_2$-L3 complex.

The Rh contents of catalysts ($Rh_2$-L*n*) (*n*=1-3) were determined by TG analysis following the procedure of Kaskel and our previous work.[1-2] Based on the residual mass at 650 °C, the rhodium (III) oxide contents of the samples are 20.8%, 16.7% and 17.7%, respectively. Therefore, the $Rh_2$ content in the $Rh_2$-L1, $Rh_2$-L2 and $Rh_2$-L3 coordination polymers is 0.82, 0.66 and 0.70 mmol/g, respectively.

**Table S1**. The $Rh_2$ content in the $Rh_2$-L*n* (*n*=1-3) catalysts.

| Sample | $Rh_2$-L1 | $Rh_2$-L2 | $Rh_2$-L3 |
|---|---|---|---|
| $Rh_2$ content (mmol/g) | 0.82 | 0.66 | 0.70 |

## 2. FT-IR

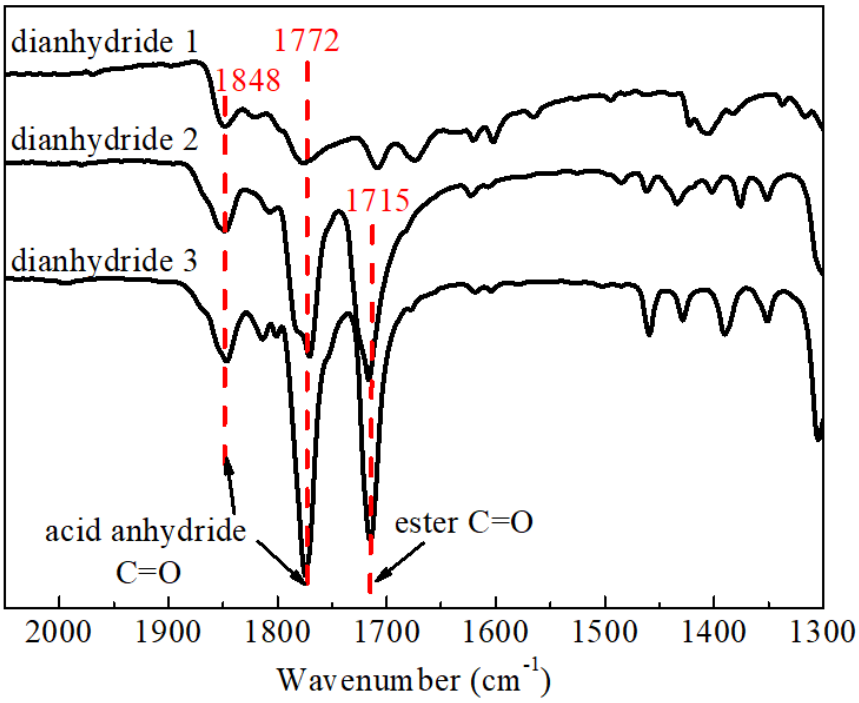


**Figure S2.** FT-IR spectra of dianhydride 1, 2 and 3.

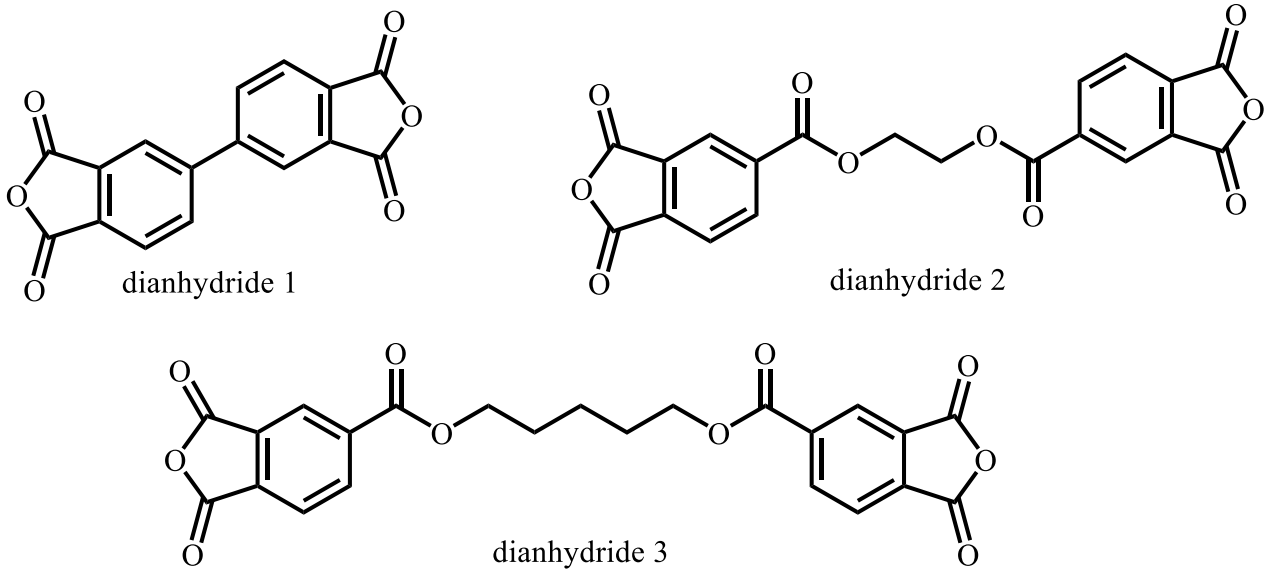


The FT-IR spectra in the range between 2050-1300 $cm^{-1}$ of dianhydride 1, 2 and 3 are depicted in Figure S2. The adsorption bands around 1848 and 1772 $cm^{-1}$ are characteristic for the C=O asymmetric and symmetric vibration of the acid anhydride moiety. The bands at around 1715 $cm^{-1}$ in the dianhydride 2 and 3 spectra are assigned to C=O vibrations of ester group.

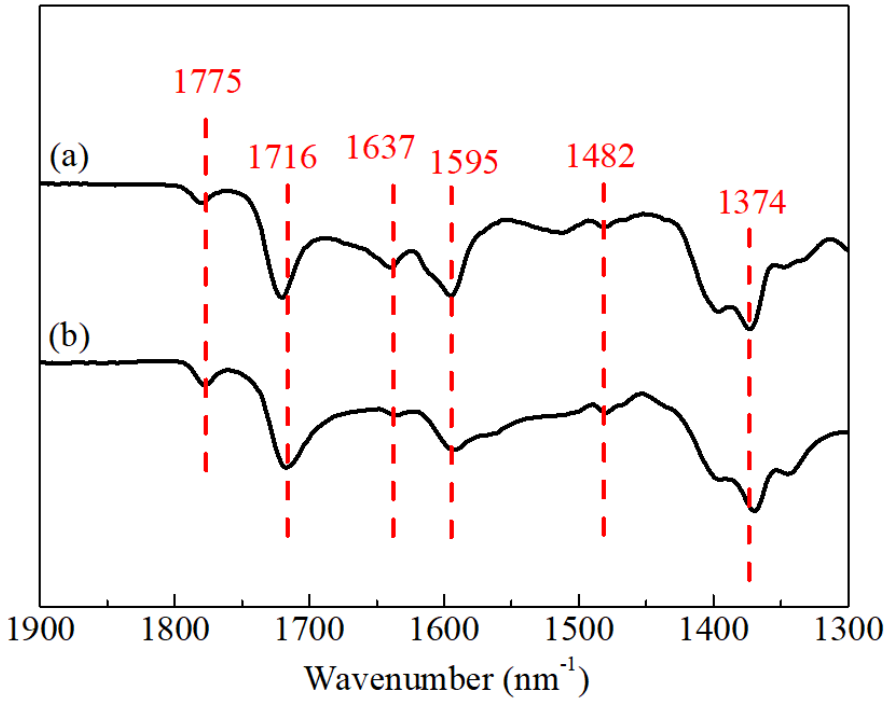


**Figure S3**. FT-IR spectra of (a) freshly prepared $Rh_2$-L3 and (b) $Rh_2$-L3 after five reaction cycles.

The FT-IR spectra in the range between 1900-1300 $cm^{-1}$ of (a) $Rh_2$-L3 and (b) after run five times of $Rh_2$-L3 are depicted in Figure S3. The adsorption bands around 1775 and 1716 $cm^{-1}$ are characteristic for the C=O asymmetric and symmetric vibration of the imide moiety. The C=O of the carboxylate is visible as signals at 1595 $cm^{-1}$ (symmetric stretching vibration) and 1637 $cm^{-1}$ (asymmetric stretching vibration). The bands at around 1482 and 1374 $cm^{-1}$ are assigned to C=C vibrations of aromatic rings and C-N stretching vibrations, respectively. No significant differences in the spectra patterns are obtained which leads to the conclusion that the structure of the $Rh_2$-L3 catalyst is preserved after catalytic reaction.

## 3. Quantitative Analysis of solid-state $^{19}$F NMR

The contents of fluorine in $Rh_2$-L*n* (*n*=1-3) polymers were calculated from solid-state $^{19}$F NMR measurements according to our previous work.[2] The $^{19}$F signals for the trifluoroacetate groups in $Rh_2$-L*n* (*n*=1-3) polymers appear at around -74 ppm. Other signals in the $^{19}$F NMR spectra are ascribed to $BaF_2$. The integral area of the NMR signal is proportional to the number of NMR active nuclei in the sample. Thus, the fluorine content in the $Rh_2$-L*n* (*n*=1-3) polymers were calculated according to the following procedure. The initial amounts of samples for measuring $^{19}$F MAS NMR are shown in Table S2. First, a mixture of the coordination polymer $Rh_2$-L1, $Rh_2$-L2 or $Rh_2$-L3, respectively, and $BaF_2$ as a standard was prepared. A specific amount of this mixture (called sample) was then filled in the rotor for measurements.

**Table S2**. Initial amounts used to prepare the samples

| **$Rh_2$-L1** | | **$Rh_2$-L2** | | **$Rh_2$-L3** | |
|---|---|---|---|---|---|
| **Masses (m) to prepare the mixtures of coordination polymer and $BaF_2$ /(g)** | | | | | |
| $Rh_2$-L1 | 0.0280 | $Rh_2$-L2 | 0.0280 | $Rh_2$-L3 | 0.0343 |
| $BaF_2$ | 0.0051 | $BaF_2$ | 0.0102 | $BaF_2$ | 0.0059 |
| $Rh_2$-L1+$BaF_2$ | 0.0331 | $Rh_2$-L2+$BaF_2$ | 0.0382 | $Rh_2$-L3+$BaF_2$ | 0.0402 |
| **Masses (m) to prepare rotors for NMR measurements /(g)** | | | | | |
| Rotor+cap | 0.5164 | Rotor+cap | 0.5166 | Rotor+cap | 0.5164 |
| Rotor+cap+sample | 0.5271 | Rotor+cap+sample | 0.5402 | Rotor+cap+sample | 0.5365 |
| Sample | 0.0107 | Sample | 0.0236 | Sample | 0.0201 |

**<u>$Rh_2$-L1:</u>**

The mass of $BaF_2$ in the sample is:

$$m_{\mathrm{BaF_2}} = BaF_2\ ratio\ \times m_{sample} = \frac{0.0051\ \mathrm{g}}{0.0331\ \mathrm{g}} \times 0.0107\ \mathrm{g} = 0.0016\ \mathrm{g}$$

The mass of fluorine in $BaF_2$ in the sample is:

$$m_{F(\mathrm{BaF_2})} = \frac{m_{\mathrm{BaF_2}}}{M_{BaF_2}} \times 2 \times M_F = \frac{0.0016\ \mathrm{g}}{175.3238\ \mathrm{g{\cdot}mol^{-1}}} \times 2 \times 18.998\ \mathrm{g{\cdot}mol^{-1}} = 3.57 \times 10^{-4}\ \mathrm{g}$$

The mass of fluorine in $Rh_2$-L1 in the sample is:

$$\frac{Area_{F(\mathrm{BaF_2})}}{Area_{F(Rh_2-L1)}} = \frac{m_{F(\mathrm{BaF_2})}}{m_{F(Rh_2-L1)}} \rightarrow m_{F(Rh_2-L1)} = \frac{Area_{F(Rh_2-L1)}}{Area_{F(\mathrm{BaF_2})}} \times m_{F(\mathrm{BaF_2})}$$

$$m_{F(Rh_2-L1)} = \frac{4.05 \times 10^5}{2.95 \times 10^5} \times 3.57 \times 10^{-4}\ \text{g} = 4.90 \times 10^{-4}\ \text{g}$$

In the sample, the overall mass of $Rh_2$-L1 is:

$$m_{Rh_2-L1} = m_{sample} - m_{BaF_2} = 0.0107\ \text{g} - 0.0016\ \text{g} = 0.0091\ \text{g}$$

The fluorine ratio in $Rh_2$-L1 is:

$$\frac{m_{F(Rh_2-L1)}}{m_{Rh_2-L1}} \times 100\ \% = \frac{4.90 \times 10^{-4}\ \text{g}}{0.0091\ \text{g}} \times 100\ \% \cong 5.4\ \%$$

The fluorine content in $Rh_2$-L1 is:

$$\text{Florine content (mol·g}^{-1}\text{)} = \frac{m_{F(Rh_2-L1)}}{m_{Rh_2-L1} \times M_F} = \frac{4.90 \times 10^{-4}\ \text{g}}{0.0091\ \text{g} \times 18.998\ \text{g·mol}^{-1}}$$

$$\approx 28.3 \times 10^{-4}\ \text{mol·g}^{-1}$$

Hence, the fluorine content in the $Rh_2$-L1 coordination polymer is 2.83 mmol/g and accordingly the content of trifluoroacetate groups is 0.94 mmol/g since each trifluoroacetate group contains three fluorine atoms.

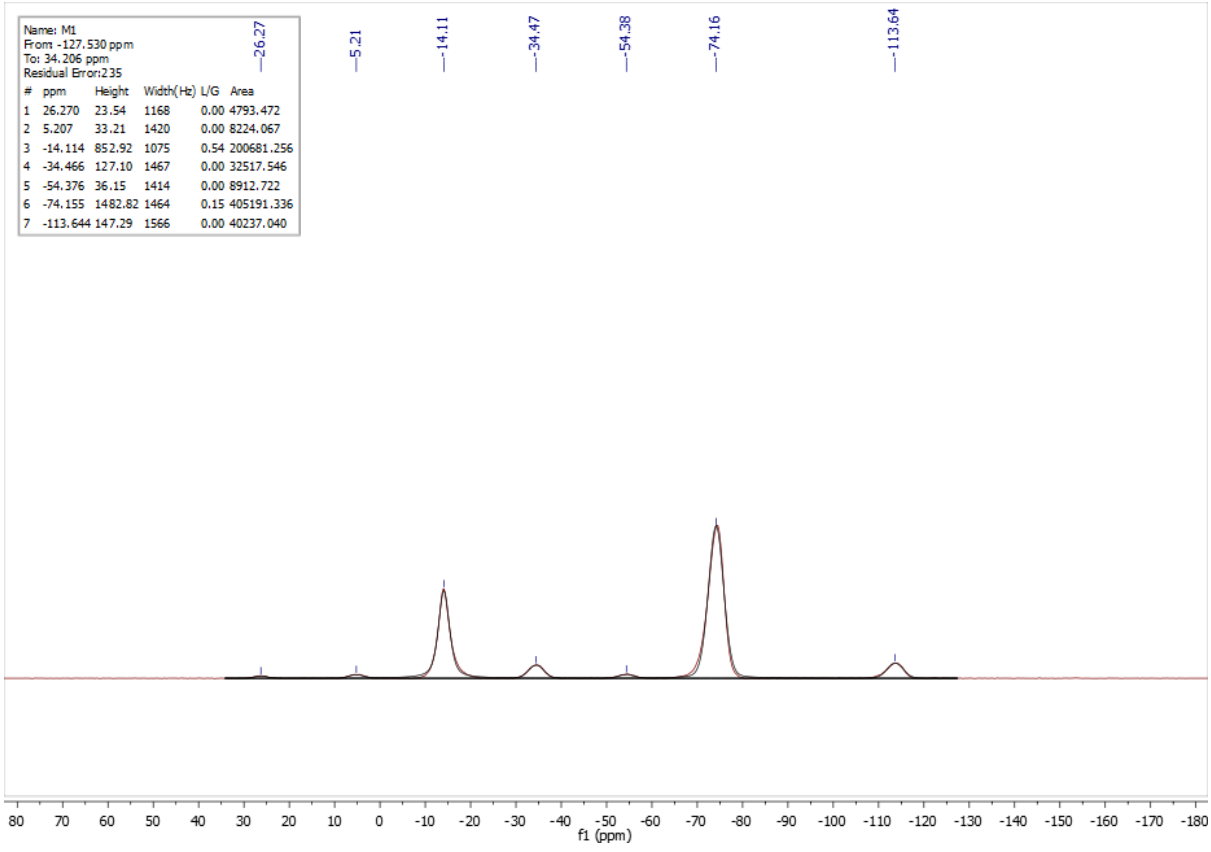

For $Rh_2$-L1, the $Rh_2$ content is 0.82 mmol/g. Thus, the $Rh_2$/TFA is 0.82/0.94=0.87, which means that on average every dirhodium unit contains one remaining TFA group. The amount of TFA groups preserved in the catalyst is 100/(0.87*4) ≈ 29 % while 71 % of the TFA groups are replaced during the formation process of the coordination polymer $Rh_2$-L1.

**$Rh_2$-L2:**

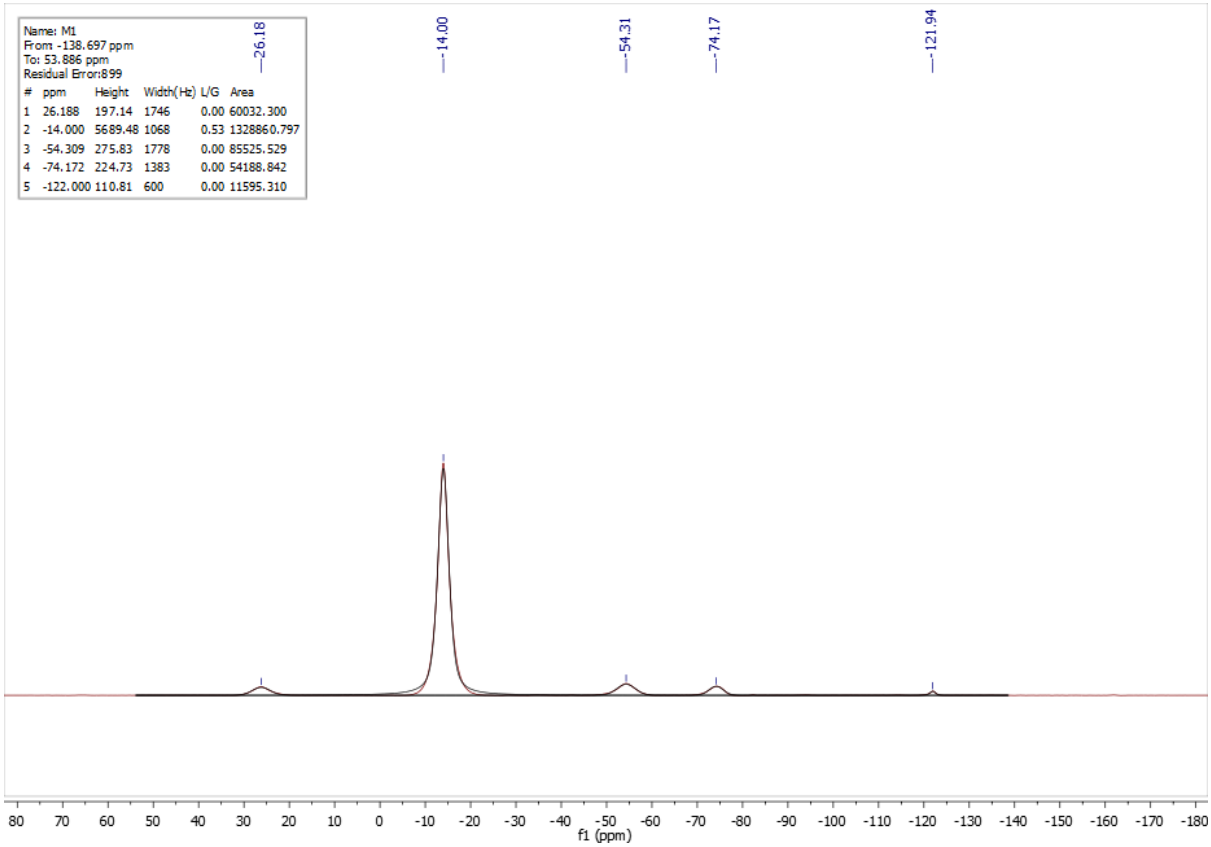


The fluorine content in the $Rh_2$-L2 coordination polymer is 0.16 mmol/g and accordingly the content of trifluoroacetate groups is 0.053 mmol/g since each trifluoroacetate group contains three fluorine atoms. For $Rh_2$-L2, the $Rh_2$ content is 0.66 mmol/g. Thus, the $Rh_2$/TFA is 0.66/0.053=12.5, which means that on average every 12.5th dirhodium unit contains one remaining TFA group. The TFA groups in the catalyst preserved are 100/(4*12.5) = 2% while 98% of the TFA groups are replaced during the formation process of the coordination polymer $Rh_2$-L2.

**$Rh_2$-L3:**

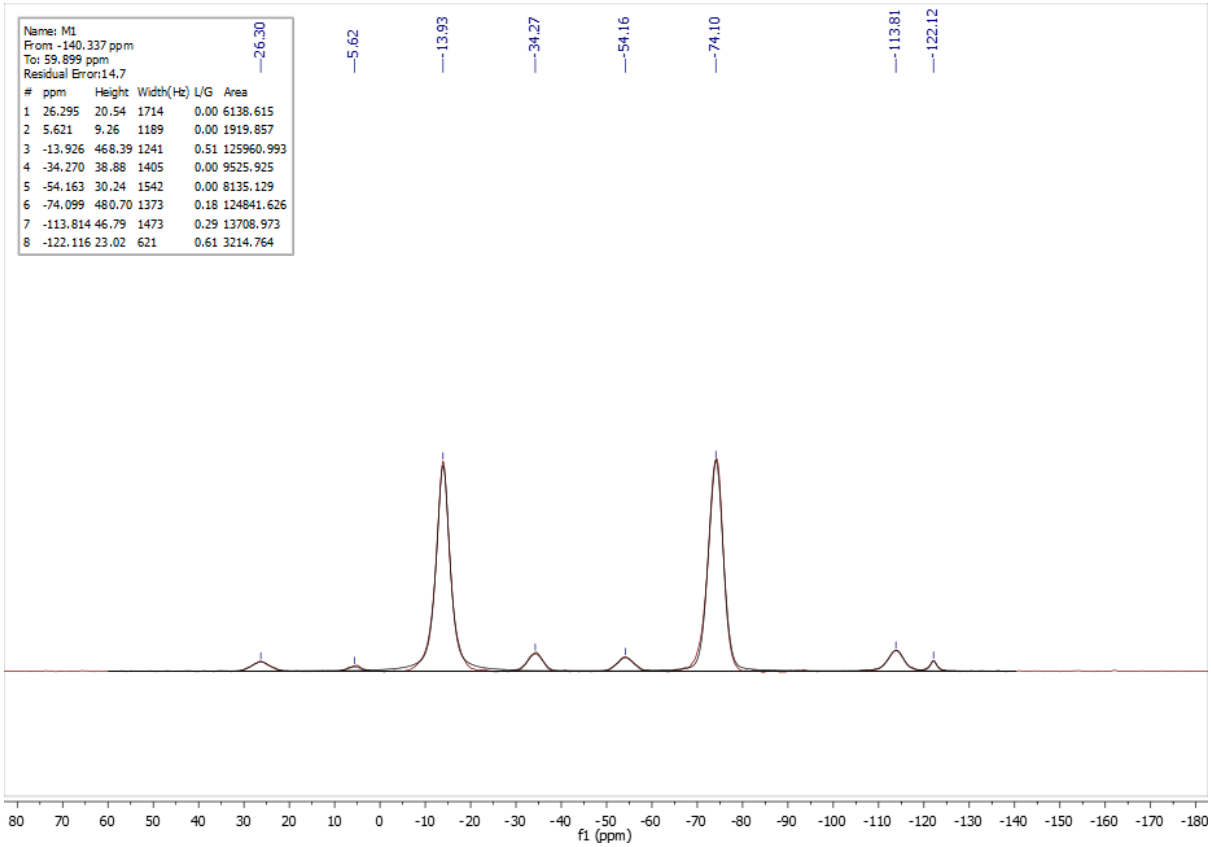


The fluorine content in the $Rh_2$-L3 coordination polymer is 1.48 mmol/g and accordingly the content of trifluoroacetate groups is 0.49 mmol/g since each trifluoroacetate group contains three fluorine atoms. For $Rh_2$-L3, the $Rh_2$ content is 0.70 mmol/g. Thus, the $Rh_2$/TFA is 0.70/0.49 ≈ 1.4, which means that on average every 1.4th dirhodium unit contains one remaining TFA group. The TFA groups in the catalyst preserved are 100/(4*1.4) ≈ 18% while 82% of the TFA groups are replaced during the formation process of the coordination polymer $Rh_2$-L3.

## 4. ICP-OES

The leaching test was performed according to a previous described procedure.[2-3] In detail, the reaction was performed at 0 ˚C. After 2 h, the catalyst was filtrated and washed with DCM at room temperature. The filtrated solution was collected for ICP-OES measurement to analyse the residual rhodium fraction. After the solvent was removed from the filtrated solution, the sample was heated at 650 ˚C for 4 h, and the residue was dissolved in 5 mL aqua regia at 50 ˚C for 24 h. Then, the sample was diluted with deionized water to obtain 25 mL solution of rhodium salts. The samples were analyzed by the AZBA GmbH, Berlin. The data of Probe I, Probe II and Probe III represent the Rh leaching of $Rh_2$-L1, $Rh_2$-L2 and $Rh_2$-L3, respectively, after the first reaction cycle. The Rh leaching for all samples is less than 0.05 ppm, which is below the detection threshold of the ICP-OES. This result suggests that the leaching of the novel dirhodium coordination polymers is negligible, which is agreement with our previous work.[2]

**Table S3.** ICP-OES for leaching solution

Probenbezeichnung: **20-07887-001: Probe I**

| Parameter | Methode | Einheit | BG | **Messwert** |
|---|---|---|---|---|
| Rhodium | DIN EN ISO 11885:2009-09 | mg/l | 0,05 | < 0,05 |

Probenbezeichnung: **20-07887-002: Probe II**

| Parameter | Methode | Einheit | BG | **Messwert** |
|---|---|---|---|---|
| Rhodium | DIN EN ISO 11885:2009-09 | mg/l | 0,05 | < 0,05 |

Probenbezeichnung: **20-07887-003: Probe III**

| Parameter | Methode | Einheit | BG | **Messwert** |
|---|---|---|---|---|
| Rhodium | DIN EN ISO 11885:2009-09 | mg/l | 0,05 | < 0,05 |

## 5. Yields

The yields in Figure 7(a) were determined by $^1$H NMR analysis of the crude reaction mixture, employing 1,3,5-trioxane as internal chemical standard. The $^1$H signal of 1,3,5-trioxane appears around 5.16 ppm, while the $^1$H signal groups at 3.37 and 3.19 ppm that refer to *trans*- and *cis*-cyclopropyloxindole, respectively. These signals were selected for the analysis. In the model reaction, 0.15 mmol of 1,3,5-trioxane was added to the crude reaction mixture, which is equal to the amount of diazooxindole employed in the reaction. Since 1,3,5-trioxane contains six equivalent protons which are represented by the intensity of the signal at 5.16 ppm and the *trans*- and *cis*- cyclopropyloxindoles each contain only one proton which is represented by the intensity of the signals at 3.37 and 3.19 ppm, respectively, the yield can be calculated as follows.

$$yield = \frac{\frac{integral\ area\ of\ trans+cis\ cyclopropyloxindole}{Integral\ area\ of\ 1,3,5-trioxane}}{\frac{1}{6}} \times 100\%$$

1,3,5-trioxane

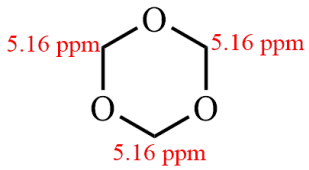


*trans*- and *cis*-cyclopropyloxindole

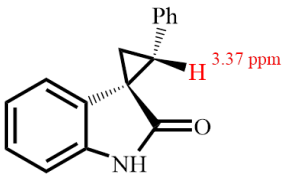


*Trans*

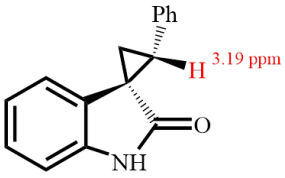


*Cis*

The yields given in Table 2 and Table 3 were determined via purification. For this the solvent of the crude reaction mixture was removed under reduced pressure. The remaining solid was purified by silica gel column chromatography (hexane/EtOAc=2:1 to 1:1) to obtain the pure cyclopropyloxindol isomers. The overall amount of *trans* and *cis*-cyclopropyloxindoles obtained from the purification step is assign to $m_1$. $m_2$ represents the theoretical amount of *trans* and *cis*-cyclopropyloxindoles obtainable when each diazooxindole is converted to cyclopropyloxindoles.

$$Purification\ yield = \frac{m_1}{m_2} \times 100\%$$

## 6. Diastereomeric Ratio (dr)

The diastereomeric ratio (dr) was determined by $^1$H NMR analysis of the crude reaction mixture according to the integral area of each signal group of $^1$H signals as dr = $area_{trans}$ : $area_{cis}$. A pair of H signals of two diastereoisomers was selected with the red color in the structure.

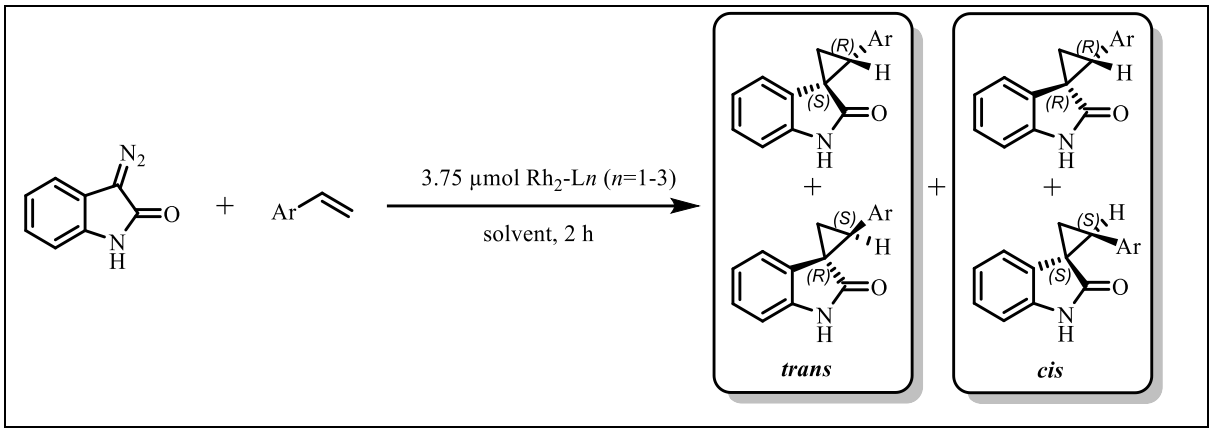


## Rh$_2$-L1 as catalyst, DCM as solvent and styrene as substrate

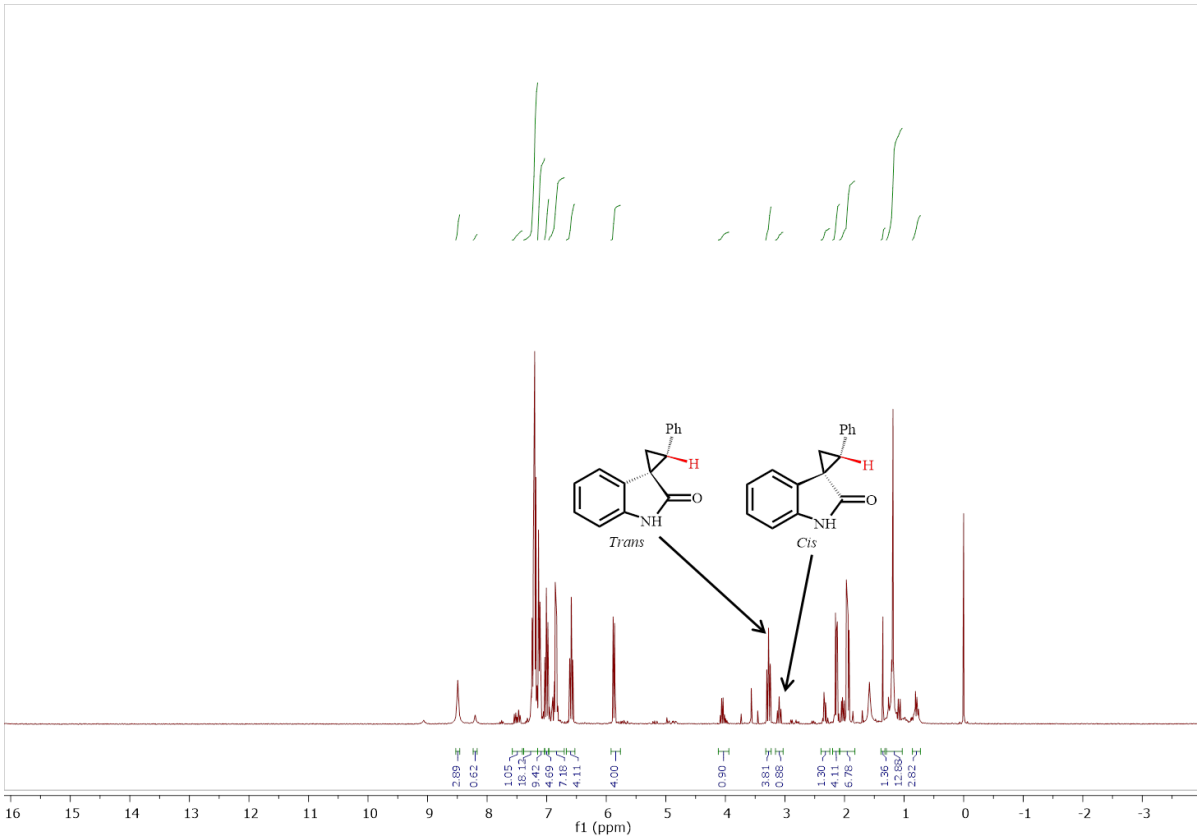


## Rh$_2$-L2 as catalyst, DCM as solvent and styrene as substrate

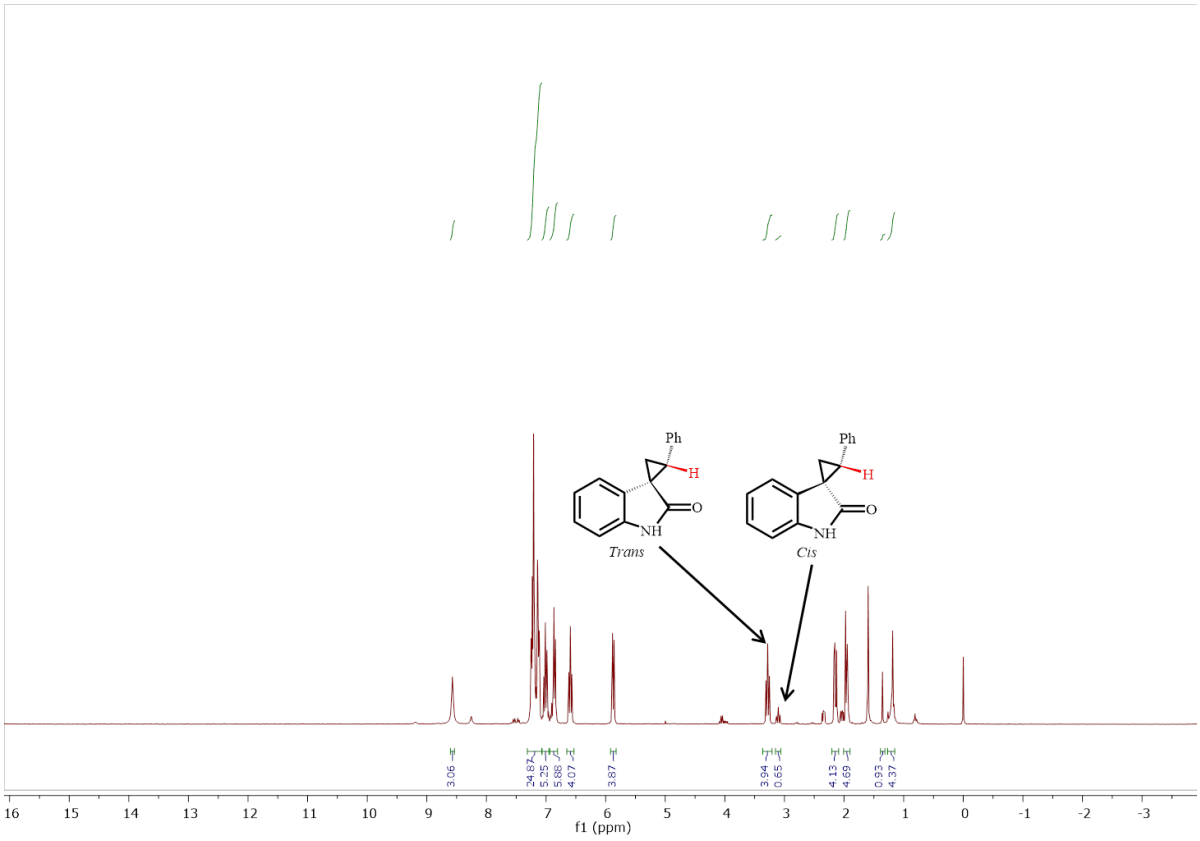


**$Rh_2$-L3 as catalyst, DCM as solvent and styrene as substrate**

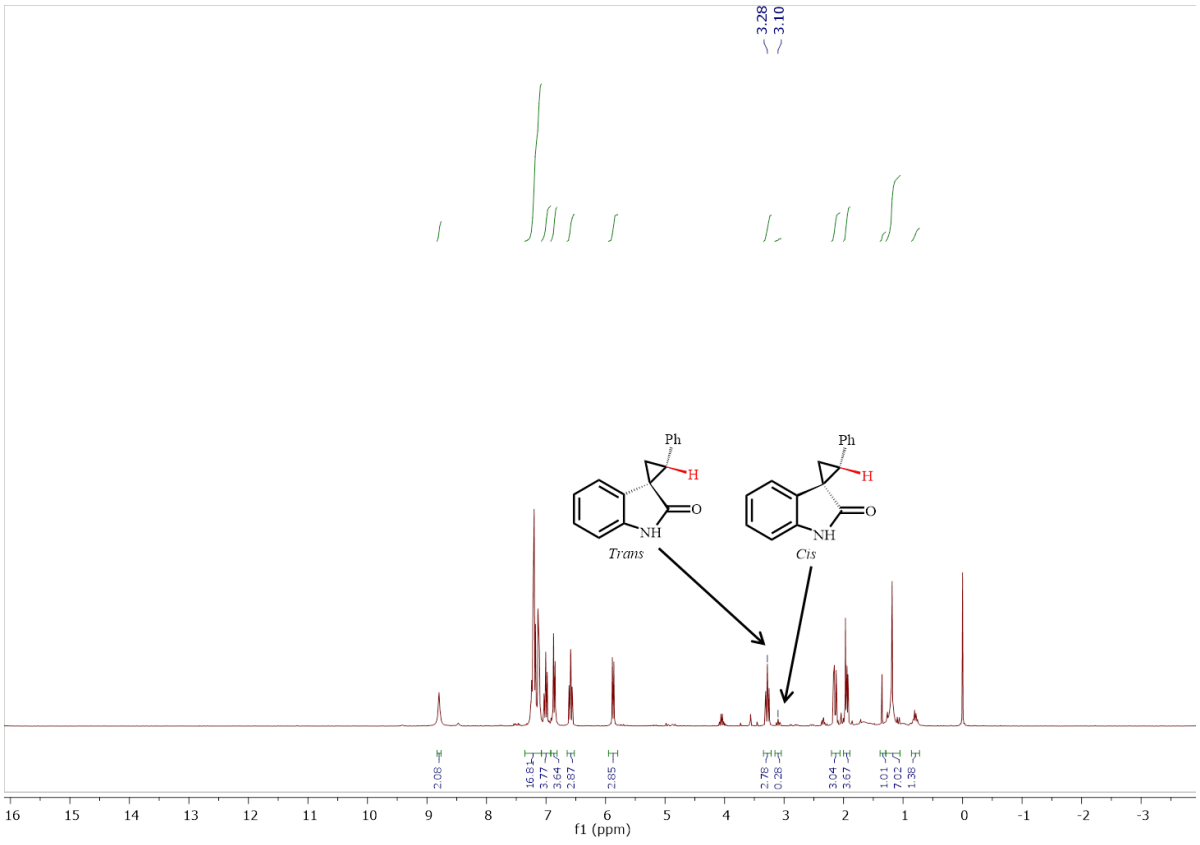


**$Rh_2$-L3 as catalyst, DCE as solvent and styrene as substrate**

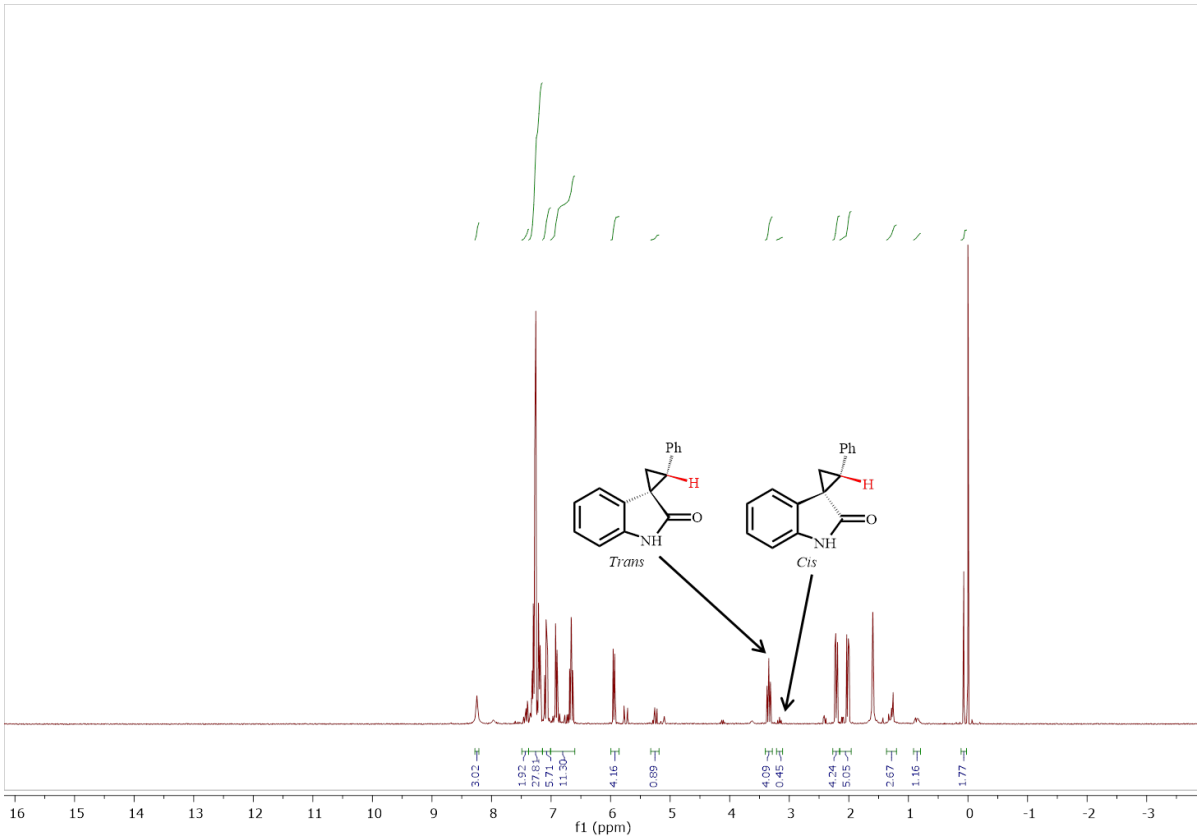


**$Rh_2$-L3 as catalyst, DCM as solvent and 4-fluorostyrene as substrate**

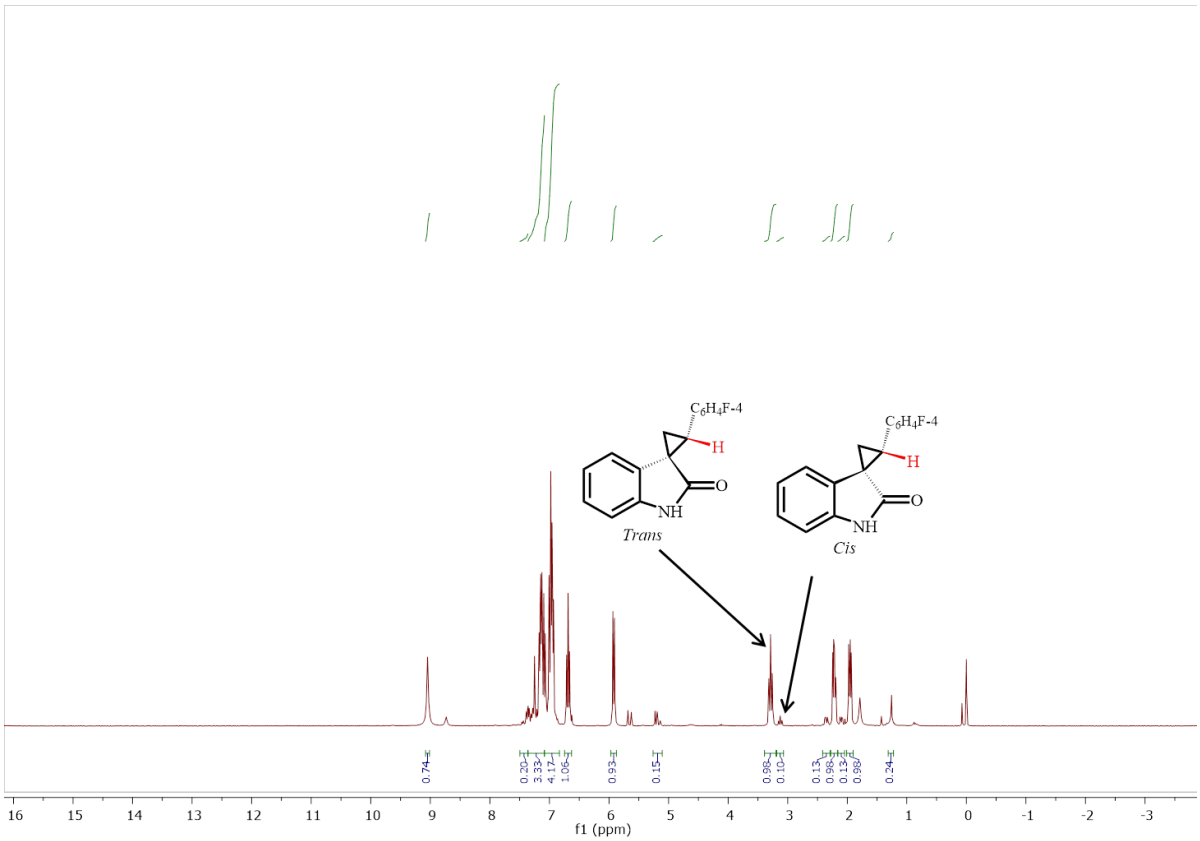


**$Rh_2$-L3 as catalyst, DCM as solvent and 4-methylstyrene as substrate**

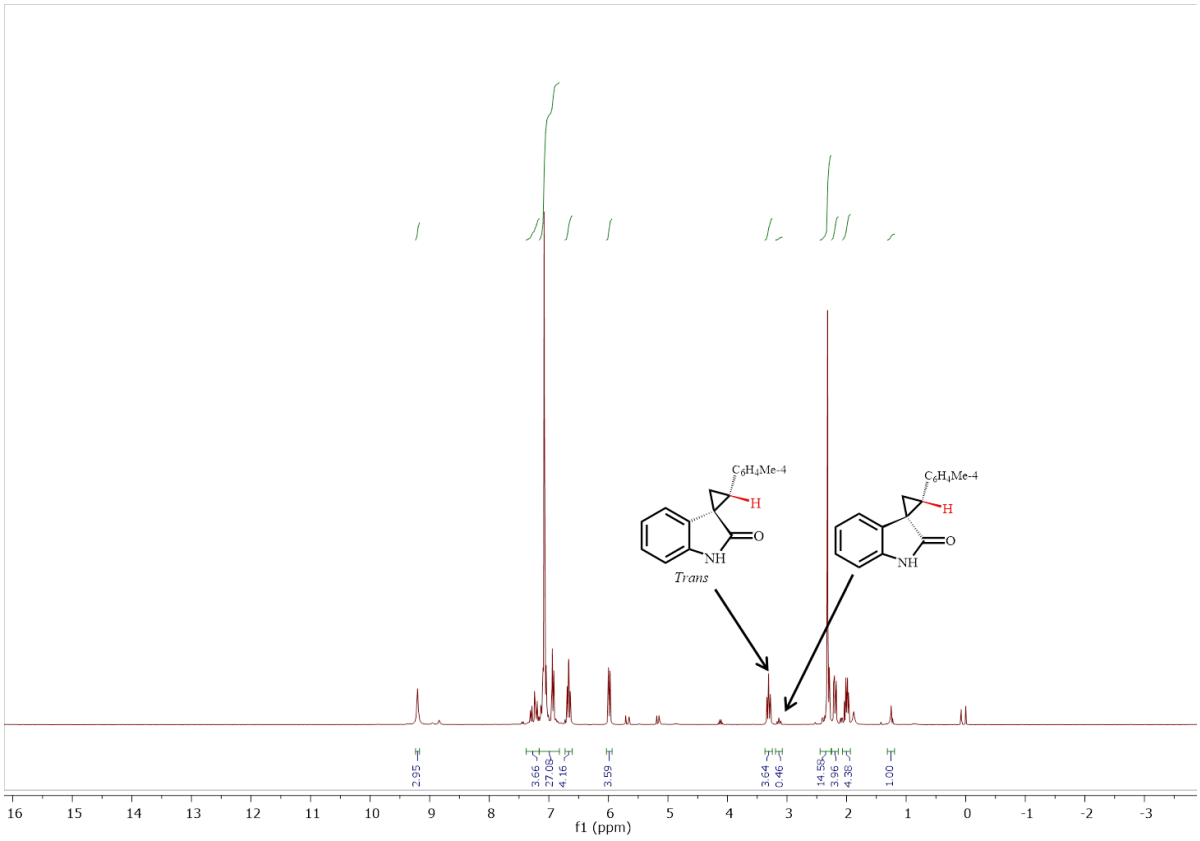


**$Rh_2$-L3 as catalyst, DCM as solvent and 4-chlorostyrene as substrate**

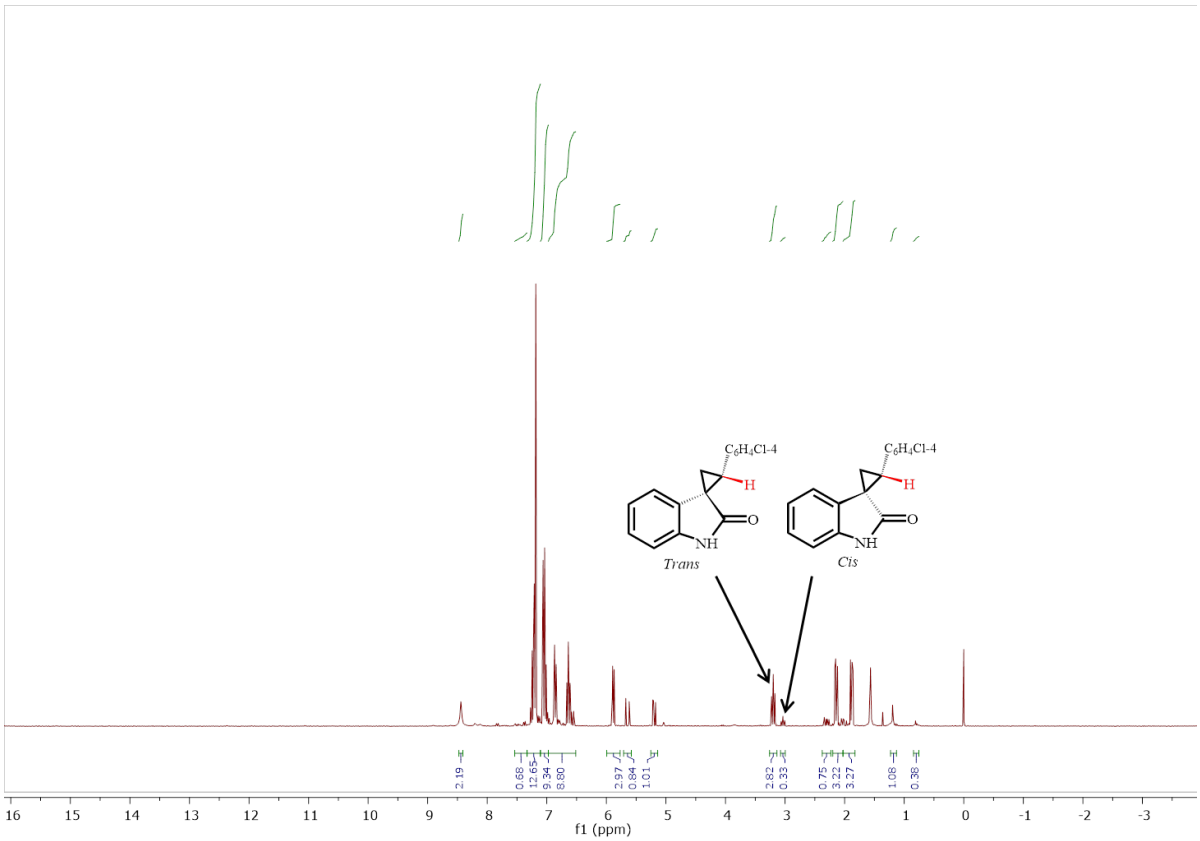


**$Rh_2$-L3 as catalyst, DCM as solvent and 4-bromostyrene as substrate**

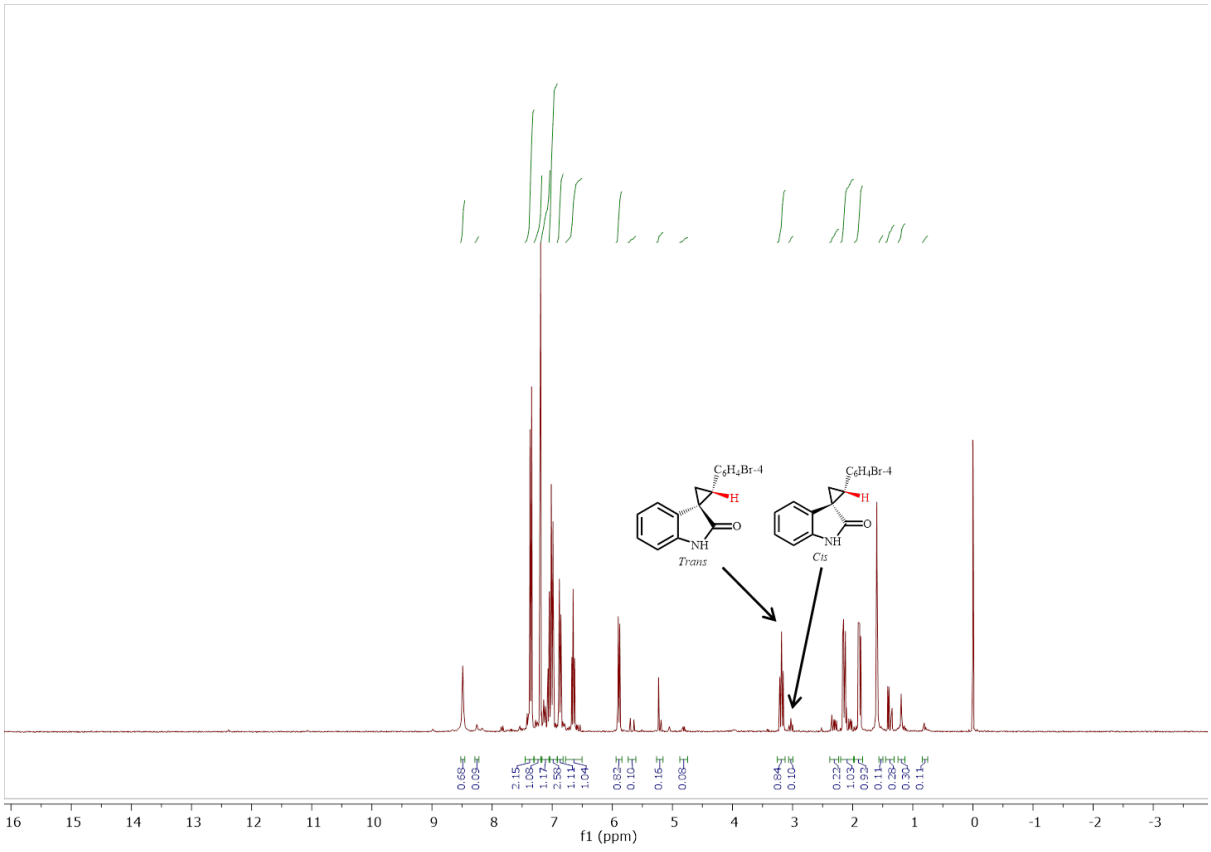
C6H4Br-4
H
O
NH
Trans
C6H4Br-4
H
O
NH
Cis
0.68
0.09
2.15
1.08
1.17
2.89
1.11
1.04
0.83
0.10
0.16
0.08
0.84
0.10
0.22
1.03
0.95
0.11
0.28
0.30
0.11
16 15 14 13 12 11 10 9 8 7 6 5 4 3 2 1 0 -1 -2 -3
f1 (ppm)

## 7. Enantiomeric excess (ee)

The enantiomeric excess (ee) for one of the *trans*-enantiomers was determined by chiral HPLC with a Reprosil chiral OM-R column [35 % MeCN in water + 0.1 % TFA, 1.0 mL/min, 70 or 110 min]. The ee % was calculated according to Eq. S1. Note: For the *cis*-enantiomers such analysis was not performed due to the small amount of these enantiomers.

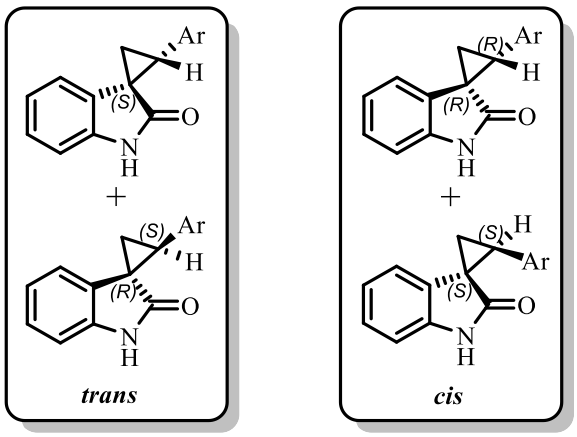


$$\text{ee } (\%) = \frac{Area_{major} - Area_{minor}}{Area_{major} + Area_{minor}} \times 100\ \% \qquad \text{Eq. S1}$$

## $Rh_2$-L1 as catalyst, DCM as solvent and styrene as substrate

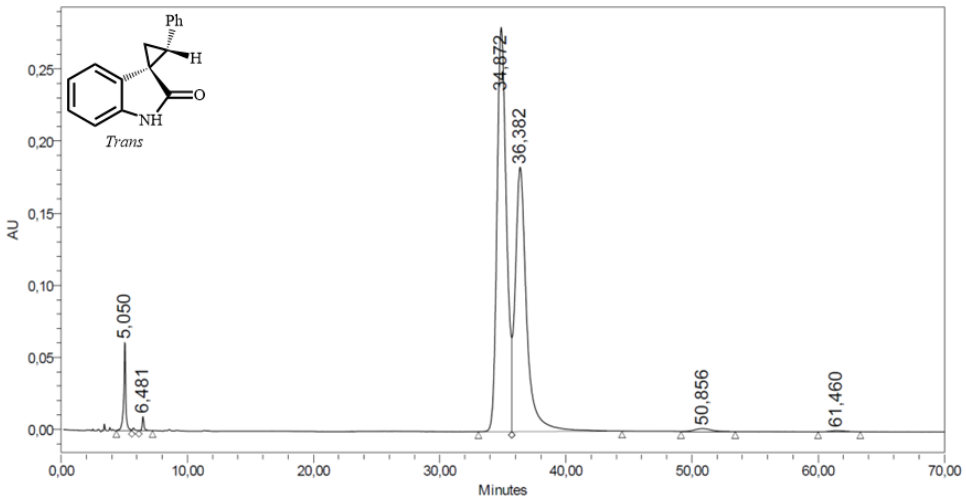


| | RT | Area | %Area | Height |
|---|---|---|---|---|
| 1 | 5,050 | 670645 | 2,47 | 61088 |
| 2 | 6,481 | 95644 | 0,35 | 9707 |
| 3 | 34,872 | 14511636 | 53,41 | 280385 |
| 4 | 36,382 | 11628113 | 42,80 | 183373 |
| 5 | 50,856 | 192562 | 0,71 | 2110 |
| 6 | 61,460 | 69818 | 0,26 | 866 |

## $Rh_2$-L2 as catalyst, DCM as solvent and styrene as substrate

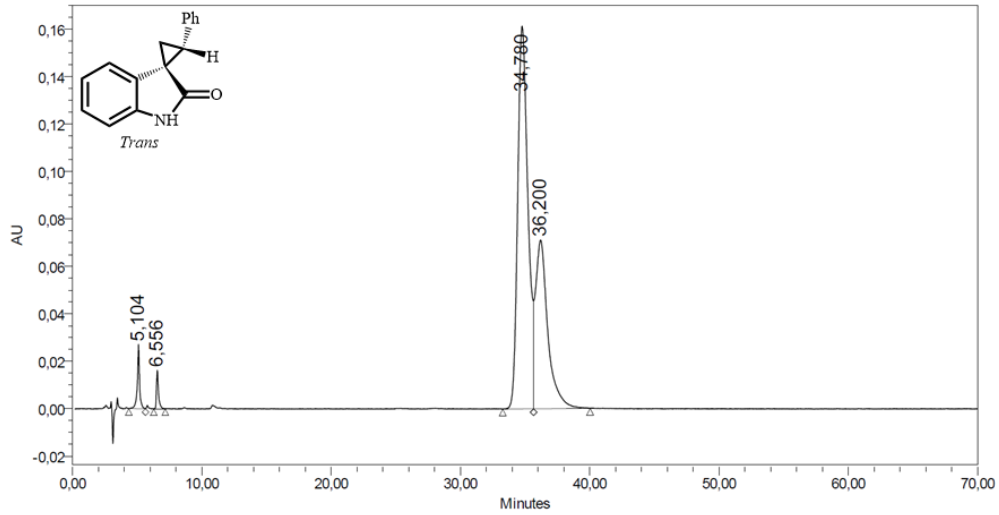


| | RT | Area | %Area | Height |
|---|---|---|---|---|
| 1 | 5,104 | 321064 | 2,28 | 27125 |
| 2 | 6,556 | 174380 | 1,24 | 16269 |
| 3 | 34,780 | 8882904 | 62,98 | 161374 |
| 4 | 36,200 | 4725786 | 33,51 | 71146 |

## $Rh_2$-L3 as catalyst, DCM as solvent and styrene as substrate

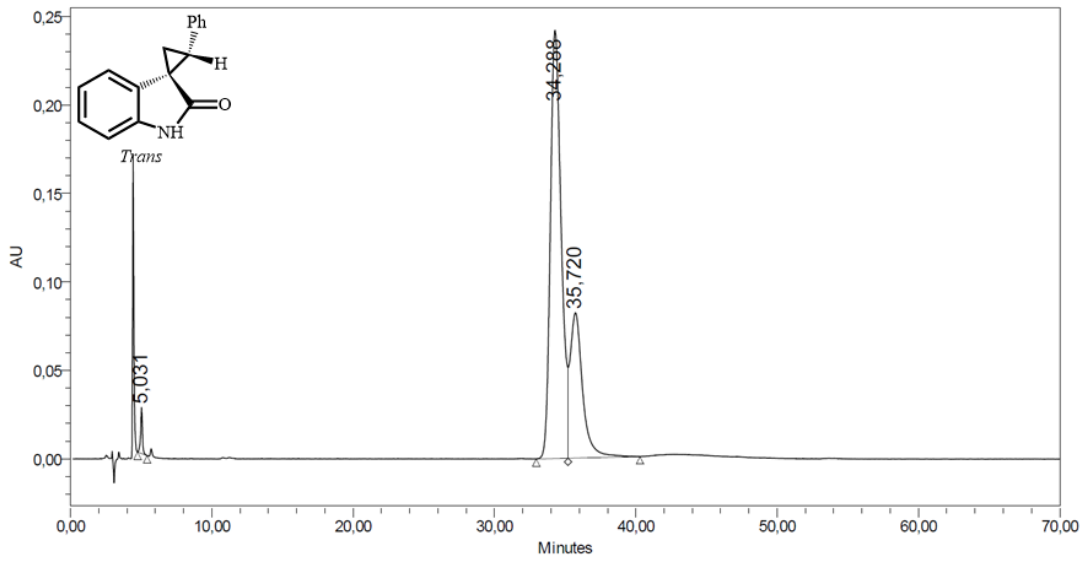


| | RT | Area | %Area | Height |
|---|---|---|---|---|
| 1 | 5,031 | 228893 | 1,26 | 26062 |
| 2 | 34,288 | 12845769 | 70,59 | 241927 |
| 3 | 35,720 | 5123308 | 28,15 | 82152 |

## $Rh_2$-L3 as catalyst, DCE as solvent and styrene as substrate

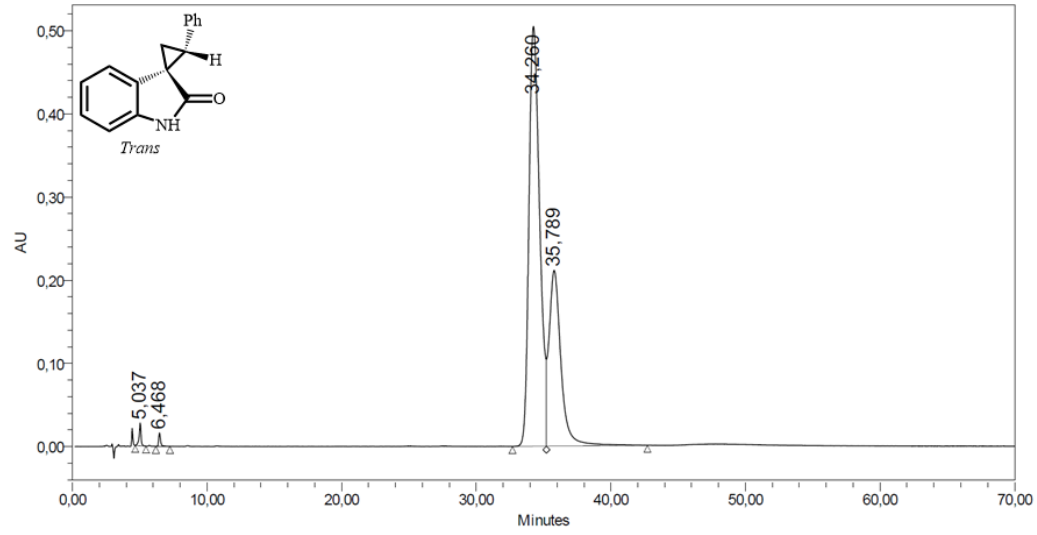


| | RT | Area | %Area | Height |
|---|---|---|---|---|
| 1 | 5,037 | 265359 | 0,64 | 27611 |
| 2 | 6,468 | 157990 | 0,38 | 16179 |
| 3 | 34,260 | 27913643 | 67,21 | 504680 |
| 4 | 35,789 | 13197648 | 31,78 | 211257 |

## $Rh_2$-L3 as catalyst, DCM as solvent and 4-fluorostyrene as substrate

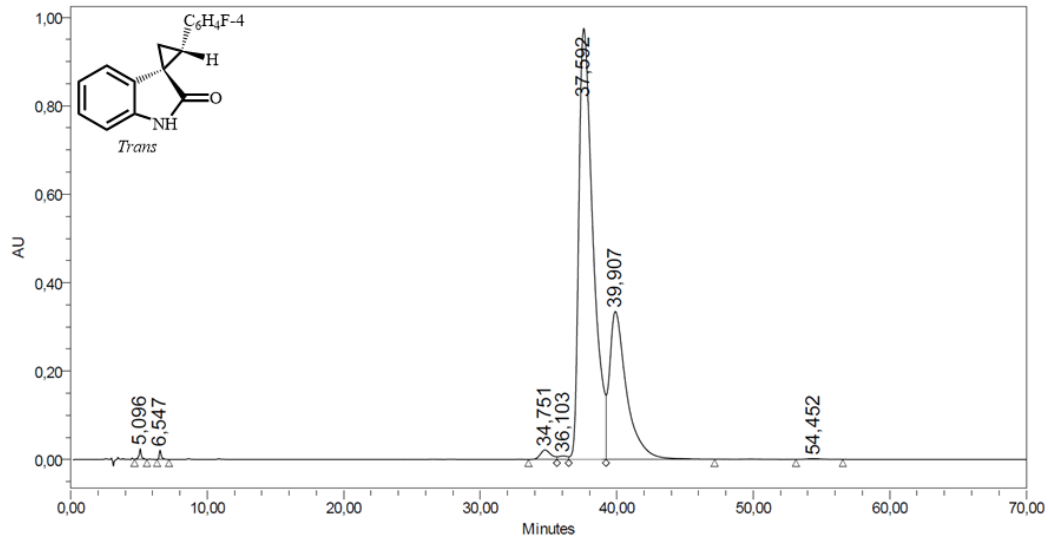


| | RT | Area | %Area | Height |
|---|---|---|---|---|
| 1 | 5,096 | 272714 | 0,27 | 23798 |
| 2 | 6,547 | 224066 | 0,22 | 20902 |
| 3 | 34,751 | 1158945 | 1,13 | 21592 |
| 4 | 36,103 | 362987 | 0,35 | 7963 |
| 5 | 37,592 | 70713308 | 69,12 | 974851 |
| 6 | 39,907 | 29449318 | 28,79 | 334698 |
| 7 | 54,452 | 124862 | 0,12 | 1514 |

## $Rh_2$-L3 as catalyst, DCM as solvent and 4-methylstyrene as substrate

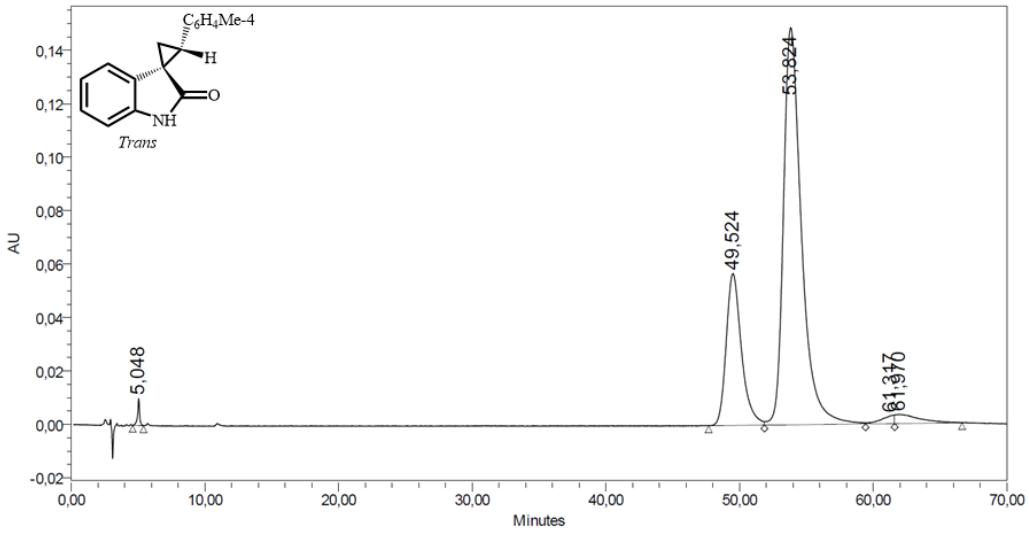


| | RT | Area | %Area | Height |
|---|---|---|---|---|
| 1 | 5,048 | 104778 | 0,55 | 10159 |
| 2 | 49,524 | 4508448 | 23,49 | 56910 |
| 3 | 53,824 | 13927914 | 72,57 | 148594 |
| 4 | 61,317 | 208014 | 1,08 | 2921 |
| 5 | 61,970 | 444531 | 2,32 | 3451 |

## $Rh_2$-L3 as catalyst, DCM as solvent and 4-clorostyrene as substrate

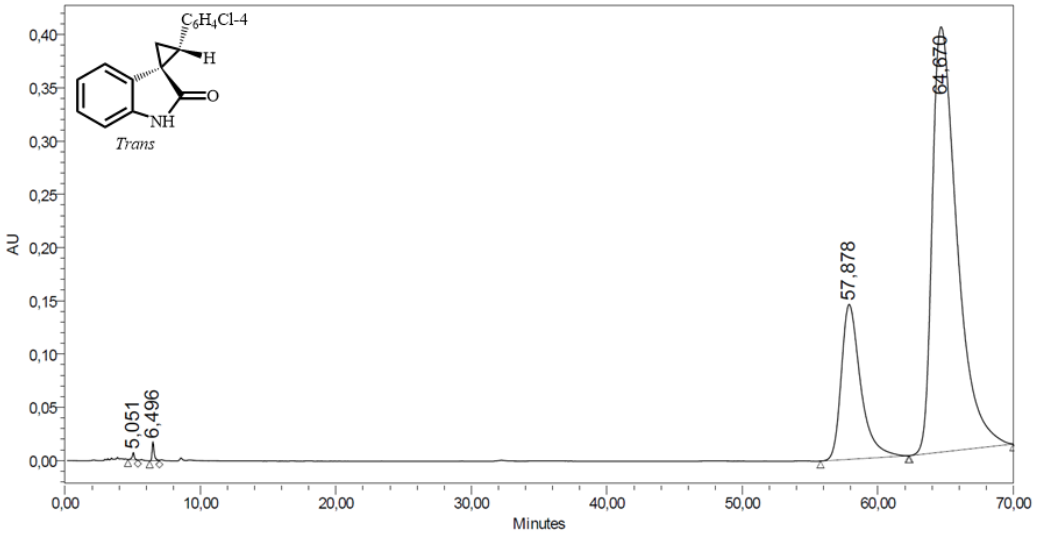


| | RT | Area | %Area | Height |
|---|---|---|---|---|
| 1 | 5,051 | 76488 | 0,12 | 6796 |
| 2 | 6,496 | 194539 | 0,30 | 17835 |
| 3 | 57,878 | 15764534 | 24,02 | 145522 |
| 4 | 64,670 | 49593344 | 75,57 | 399253 |

## $Rh_2$-L3 as catalyst, DCM as solvent and 4-bromostyrene as substrate

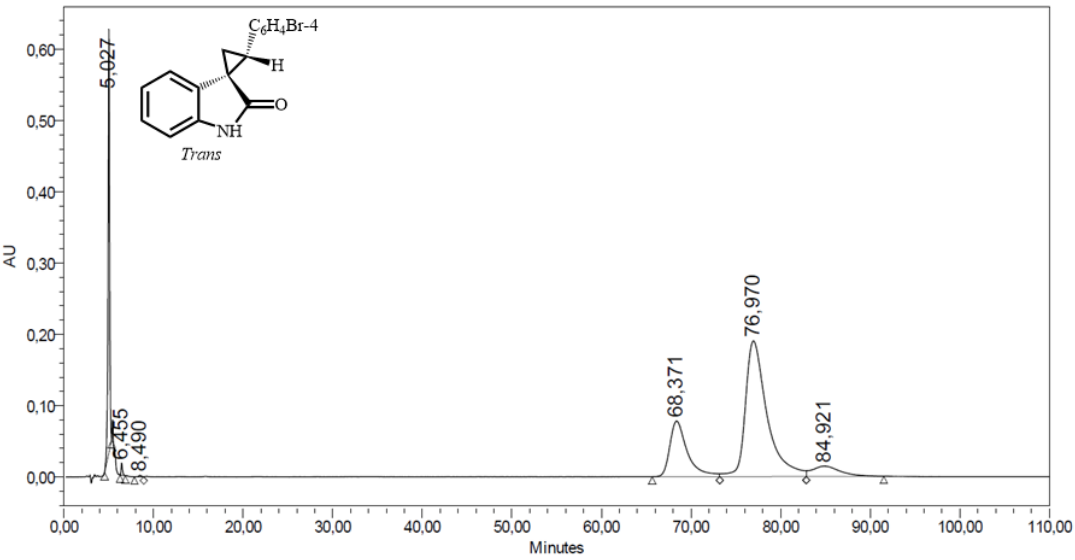


| | RT | Area | %Area | Height |
|---|---|---|---|---|
| 1 | 5,027 | 6615576 | 12,60 | 594033 |
| 2 | 6,455 | 183356 | 0,35 | 17095 |
| 3 | 8,490 | 50387 | 0,10 | 2310 |
| 4 | 68,371 | 10591371 | 20,18 | 78096 |
| 5 | 76,970 | 31886661 | 60,75 | 190460 |
| 6 | 84,921 | 3162219 | 6,02 | 14529 |

## 8. MS (ESI) Measurements

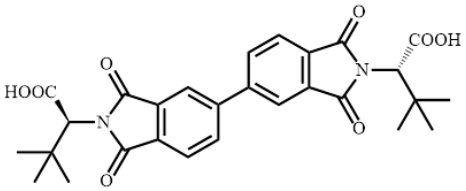


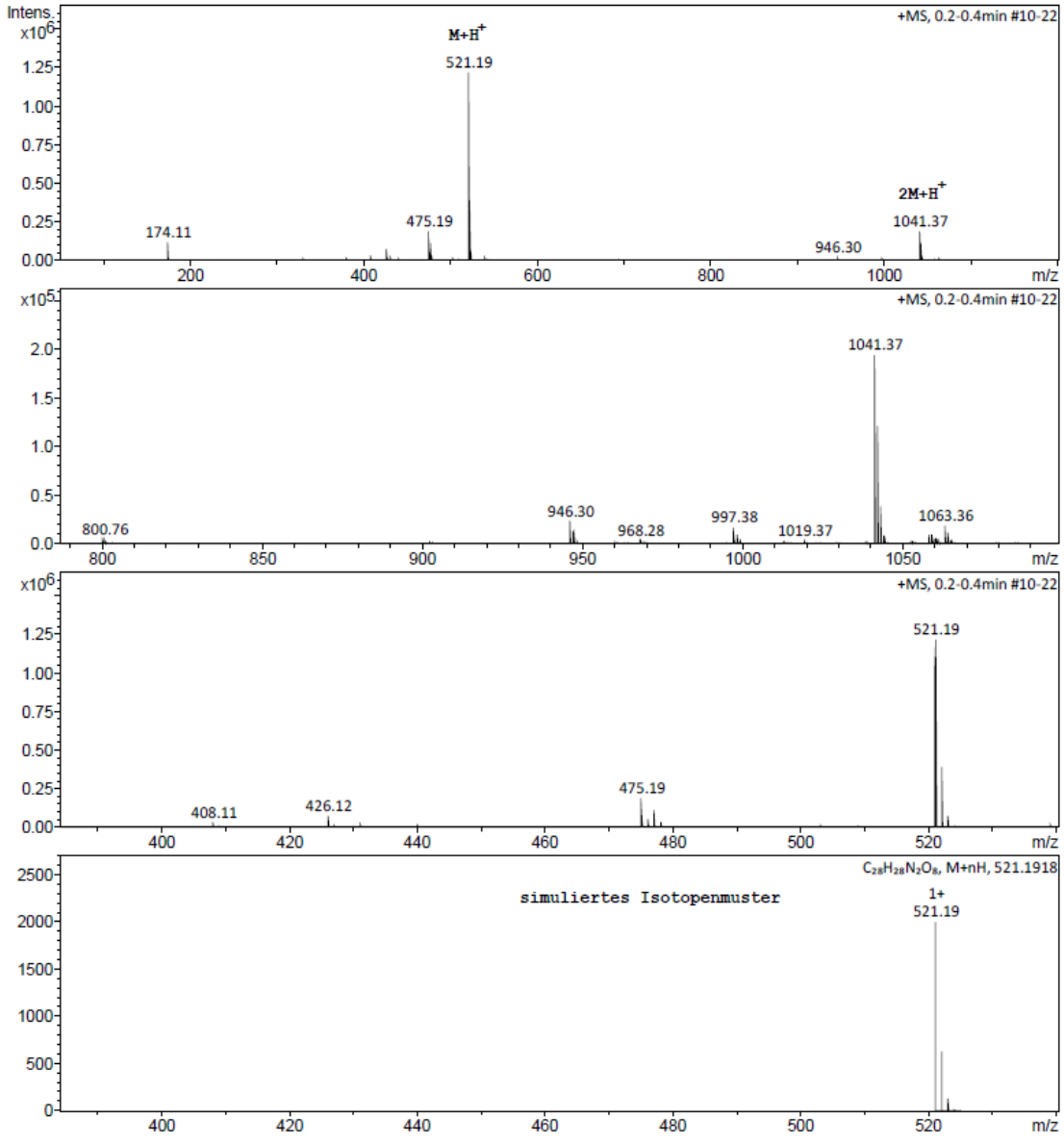


Top spectrum: Whole experimental MS spectrum. Middle two spectra: Zoom in the experimental spectrum in different spectral ranges. Bottom spectrum: simulated spectrum for the given molecular formula. MS (ESI) calc. for $C_{28}H_{29}N_2O_8$ $[M+H]^+$: 521.1879, found 521.1918. *Note*: Three peaks were observed in the simulated spectrum, which refer to $[M+H]^+$, $[M+2H]^{2+}$ and $[M+3H]^{3+}$, respectively.

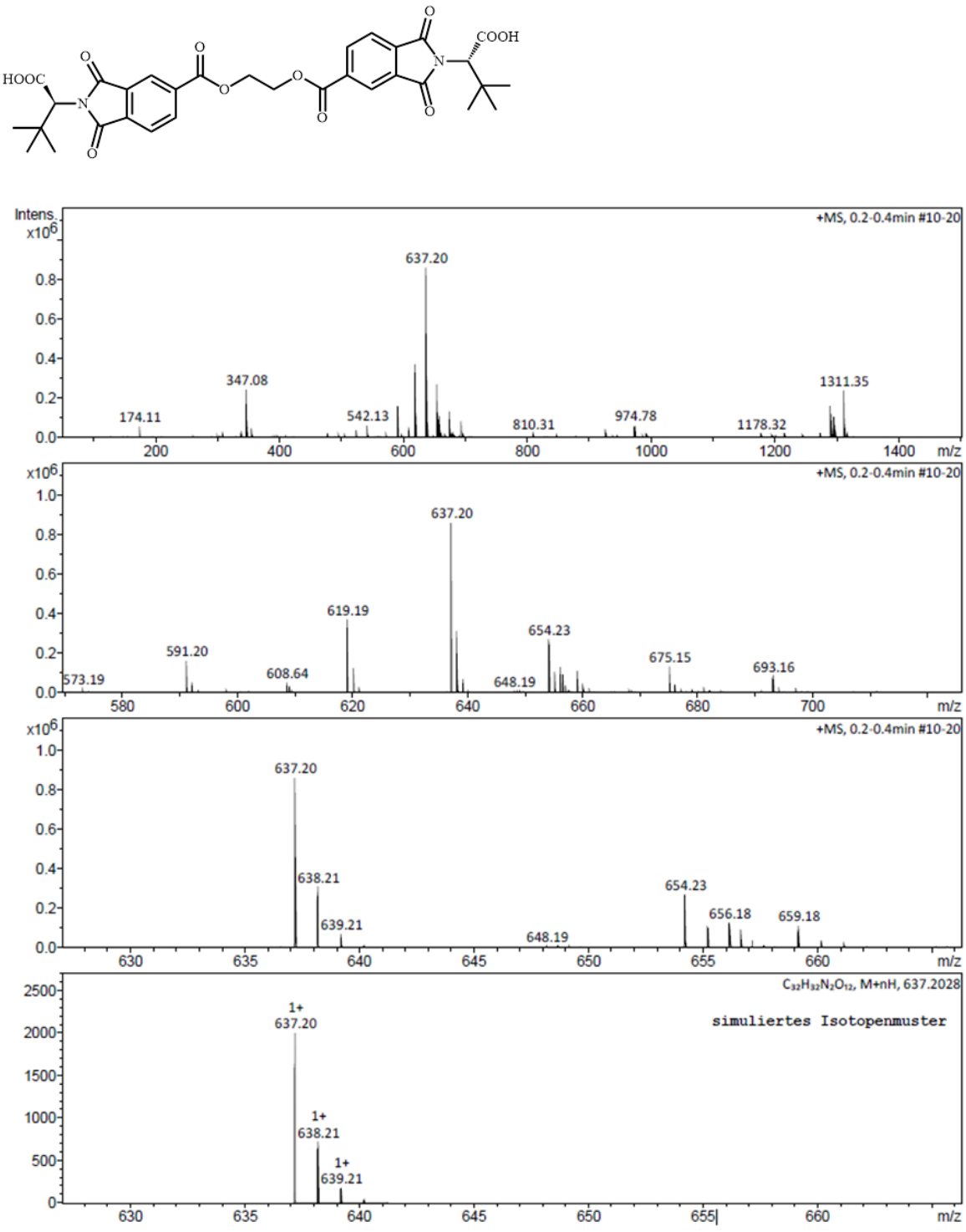


Top spectrum: Whole experimental MS spectrum. Middle two spectra: Zoom in the experimental spectrum in different spectral ranges. Bottom spectrum: Simulated spectrum for the given molecular formula. MS (ESI) calc. for $C_{32}H_{33}N_2O_{12}$ $[M+H]^+$: 637.1989, found: 637.2028. *Note*: Three peaks were observed in the simulated spectrum, which refer to $[M+H]^+$, $[M+2H]^{2+}$ and $[M+3H]^{3+}$, respectively.

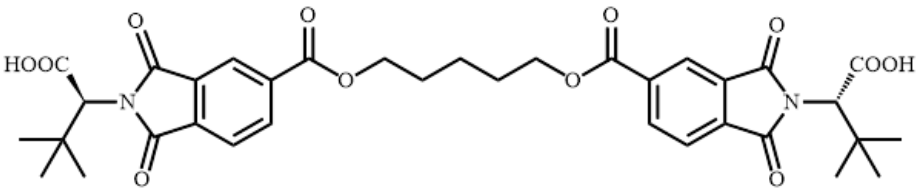


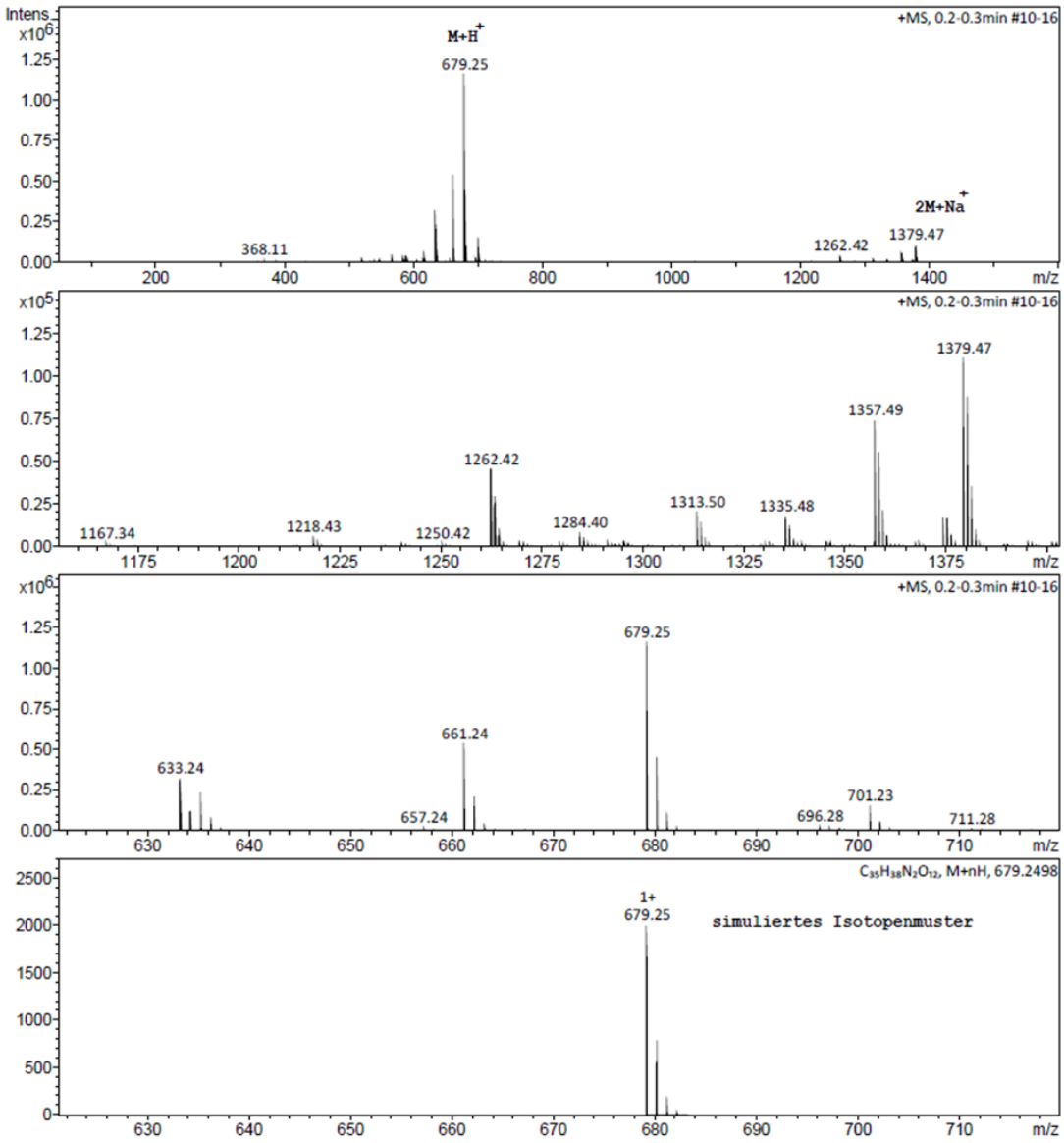


Top spectrum: Whole experimental MS spectrum. Middle two spectra: Zoom in the experimental spectrum in different spectral ranges. Bottom spectrum: Simulated spectrum for the given molecular formula. MS (ESI) calc. for $C_{35}H_{39}N_2O_{12}$ $[M+H]^+$ : 679.2458, found: 679.2498. *Note*: Three peaks were observed in the simulated spectrum, which refer to $[M+H]^+$, $[M+2H]^{2+}$ and $[M+3H]^{3+}$, respectively.

## 8. $^{1}$H NMR and $^{13}$C NMR Spectra

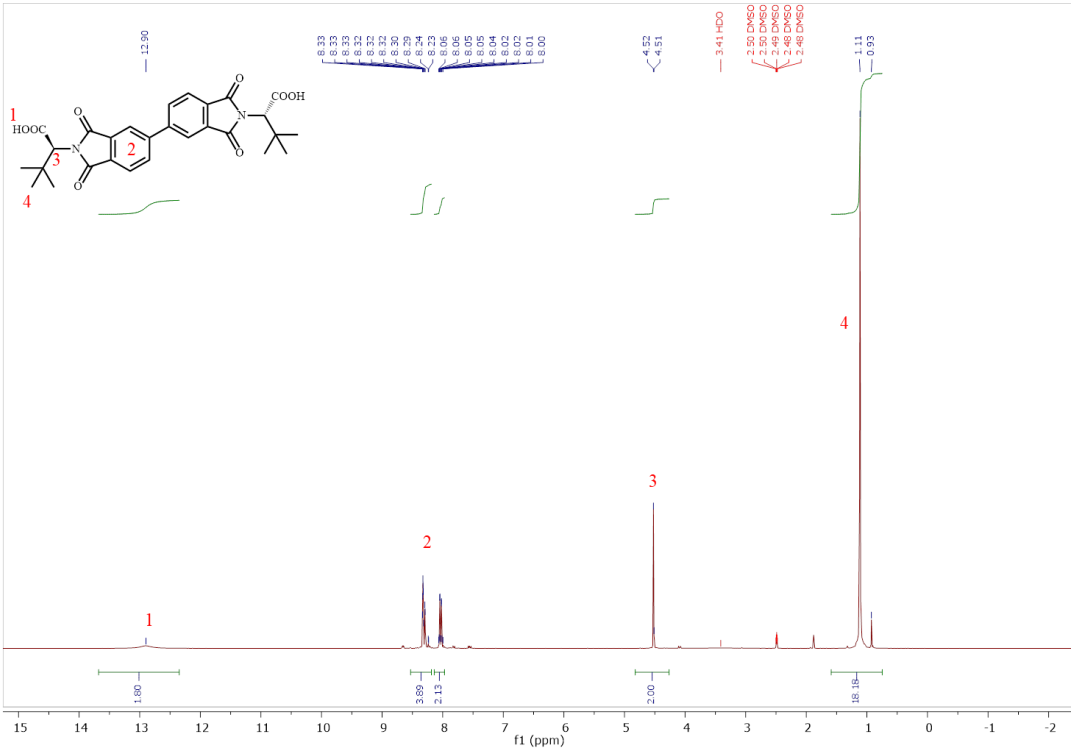


$^{1}$H NMR spectrum of $H_2L1$

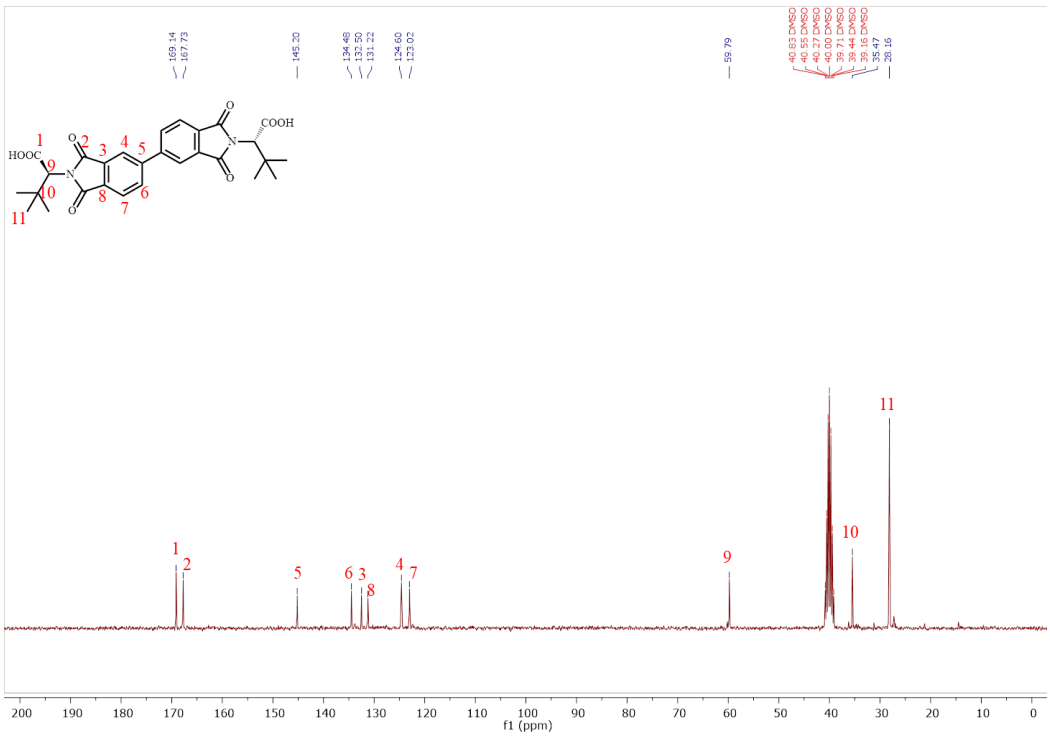


$^{13}$C NMR spectrum of $H_2L1$

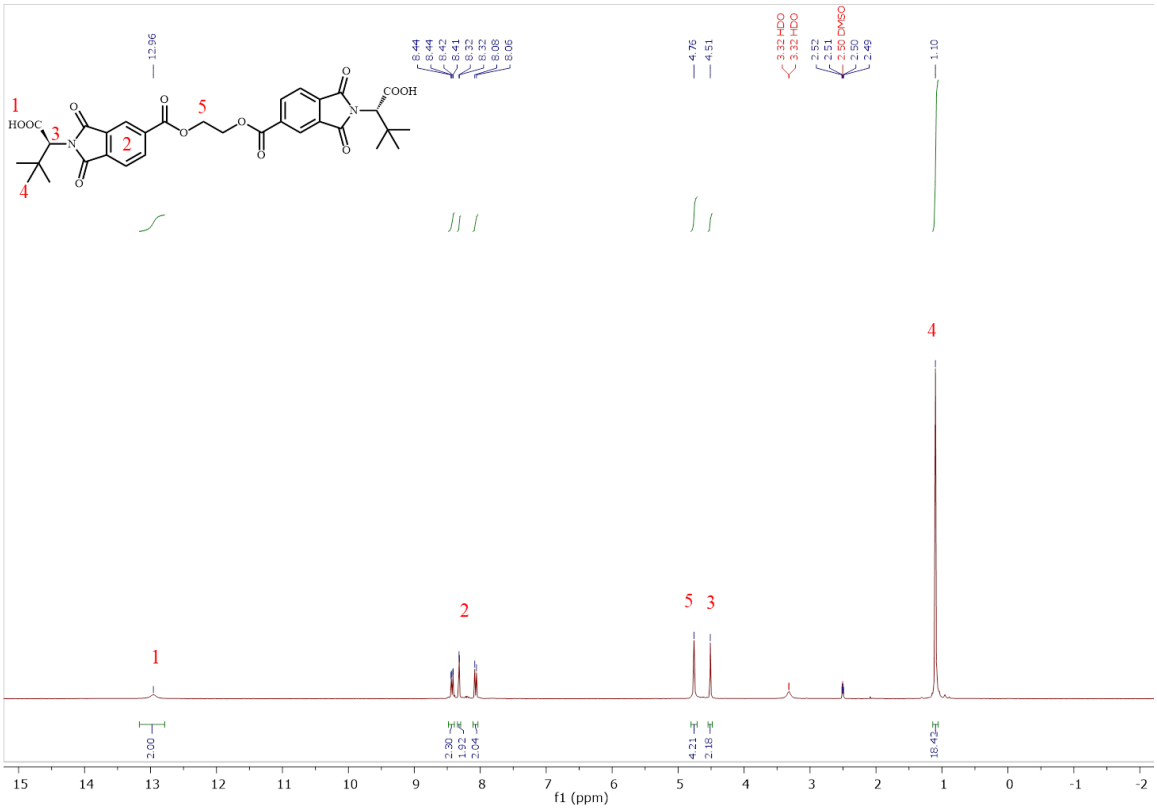


$^{1}$H NMR spectrum of $H_2L2$

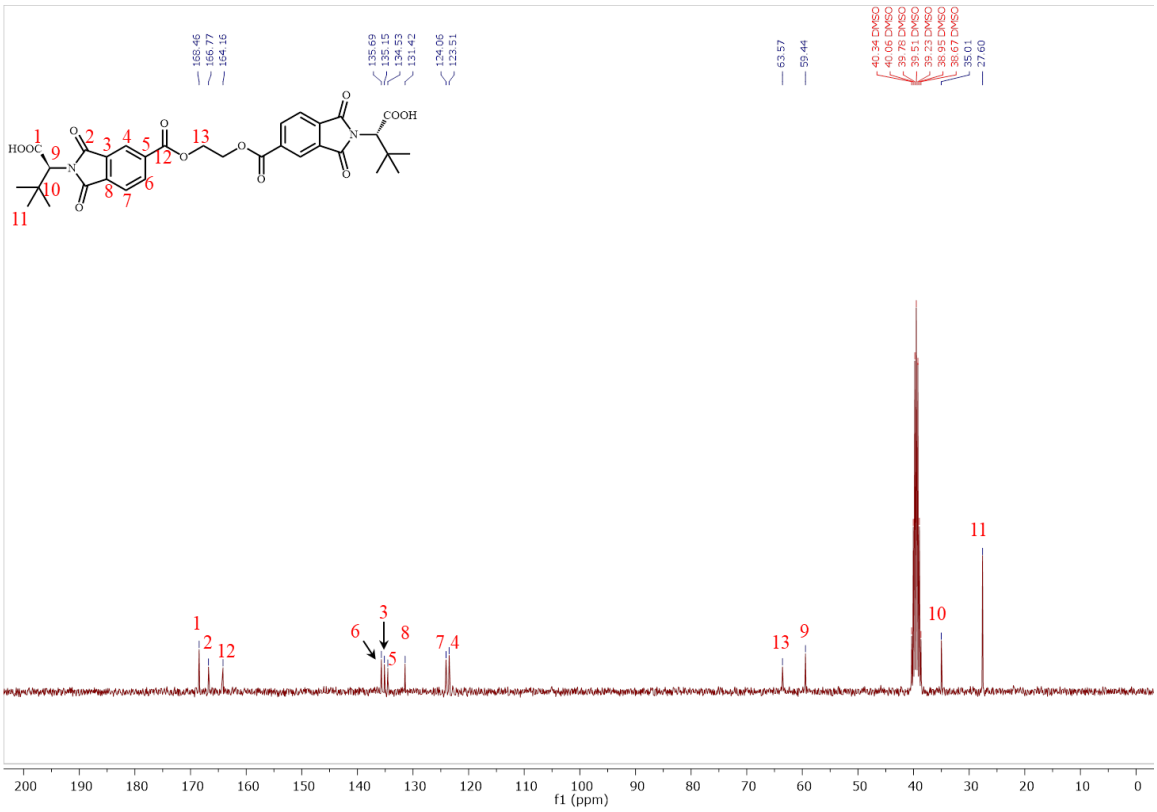


$^{13}$C NMR spectrum of $H_2L2$

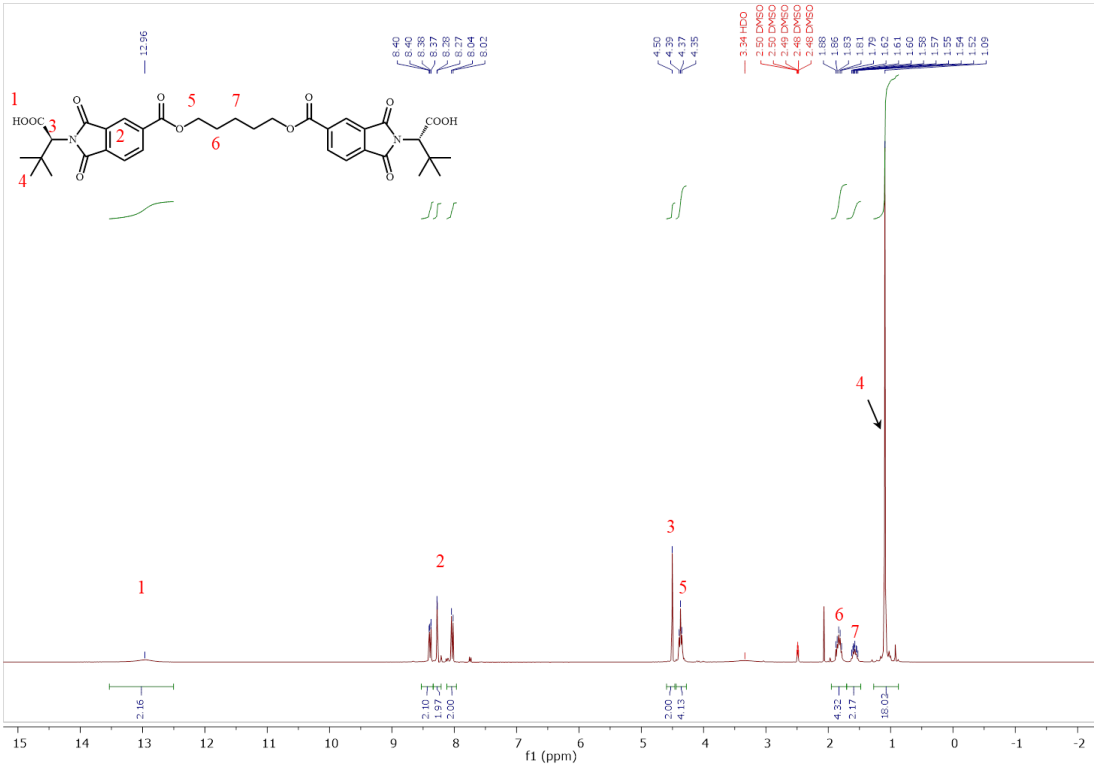


$^{1}$H NMR spectrum of $H_2$L3

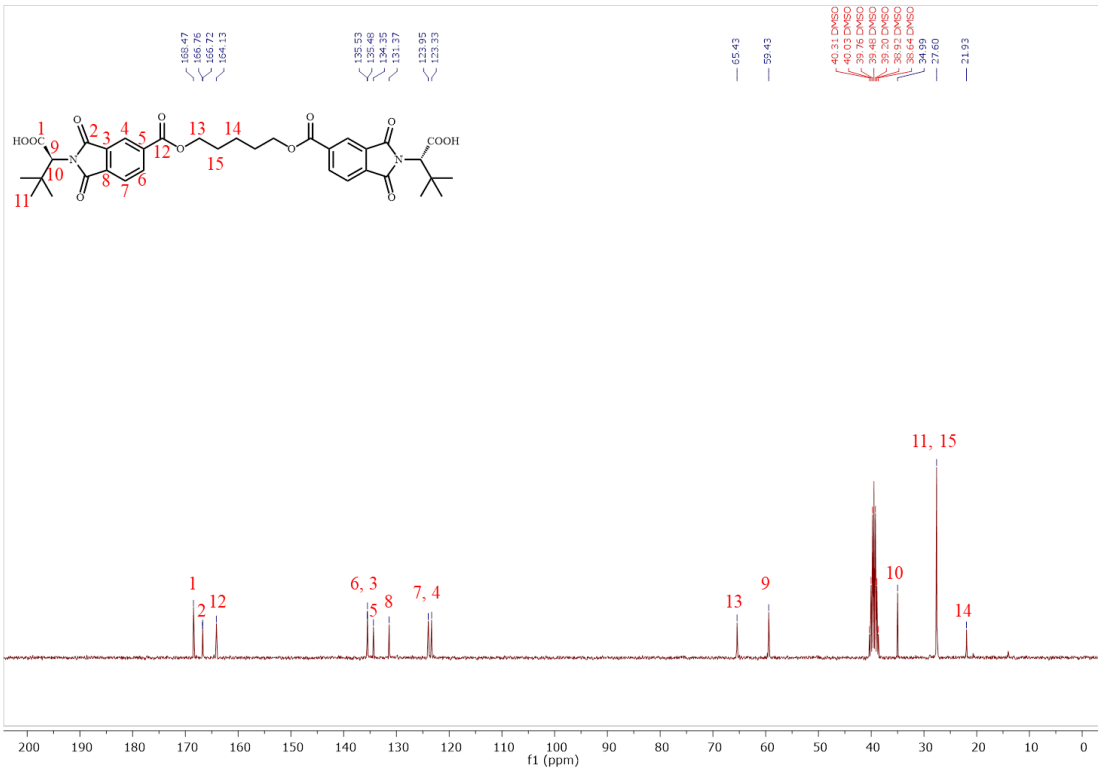


$^{13}$C NMR spectrum of $H_2$L3

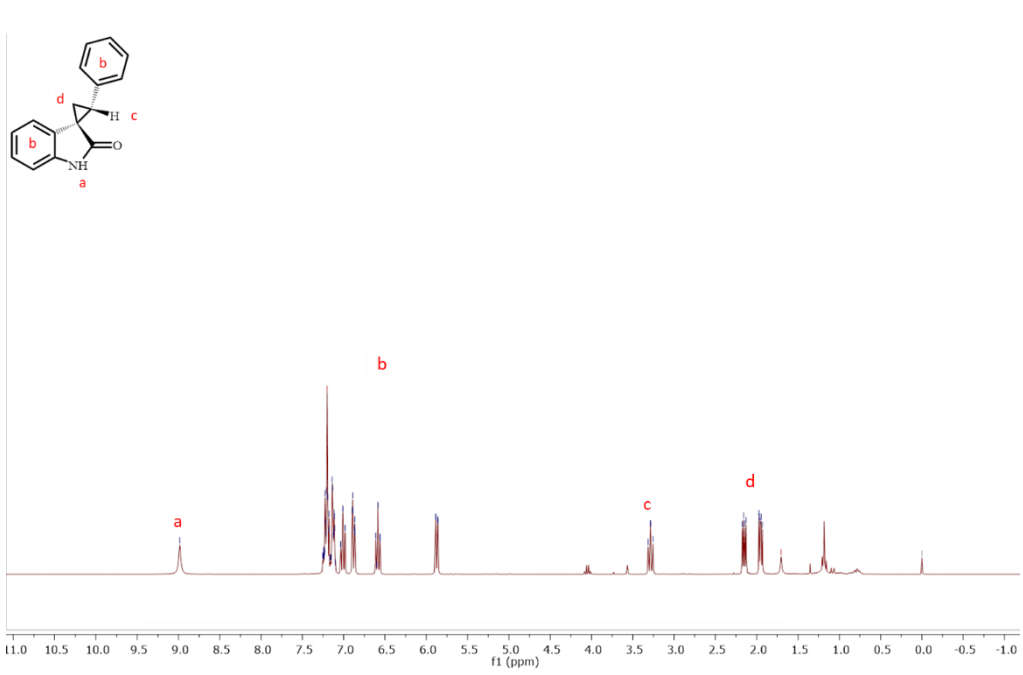


$^{1}$H NMR spectrum of 2-phenylspiro[cyclopropane-1,3'-indolin]-2'-one

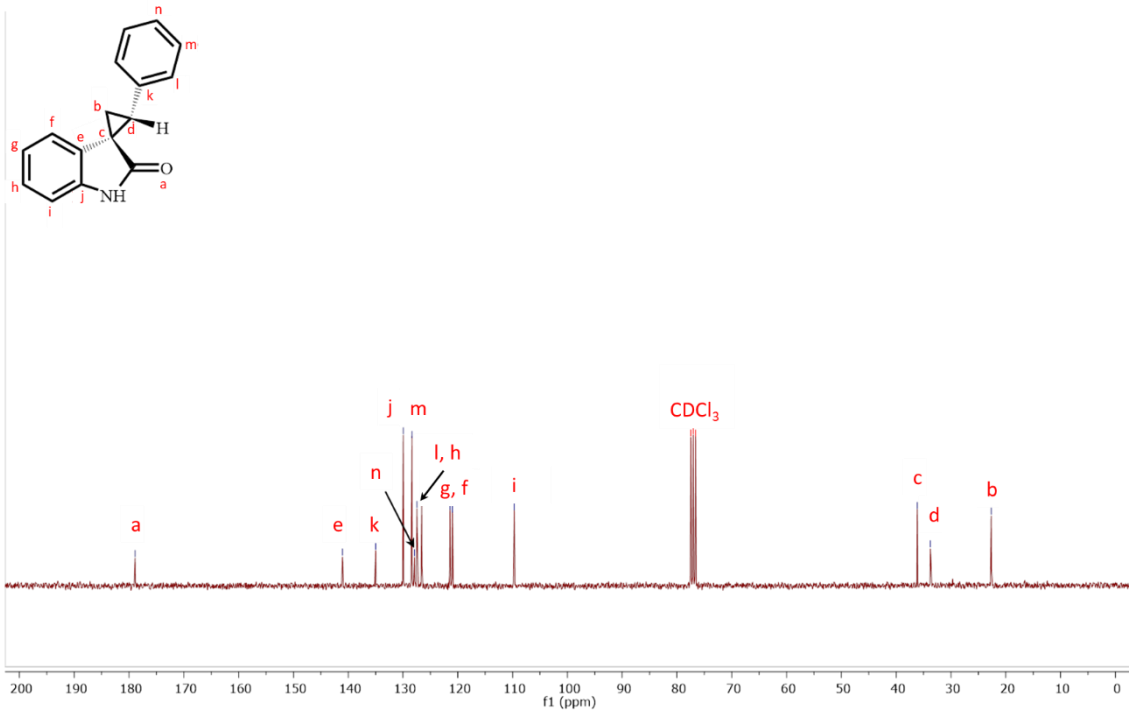


$^{13}$C NMR spectrum of 2-phenylspiro[cyclopropane-1,3'-indolin]-2'-one

*Note*: The $^{1}$H and $^{13}$C NMR spectra of 2-phenylspiro[cyclopropane-1,3'-indolin]-2'-one are adapted from reference [2]. The following spectra of products were recorded according to reference [2] and [4].

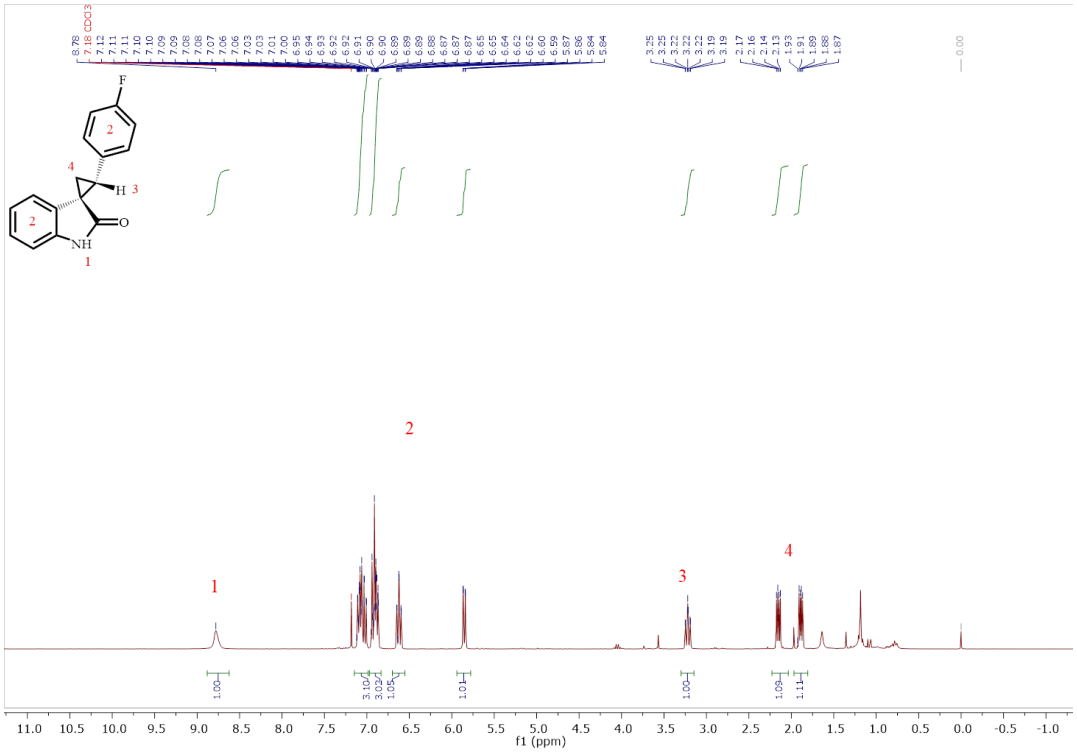


$^{1}$H NMR spectrum of 2-(4-fluorophenyl)spiro[cyclopropane-1,3'-indolin]-2'-one

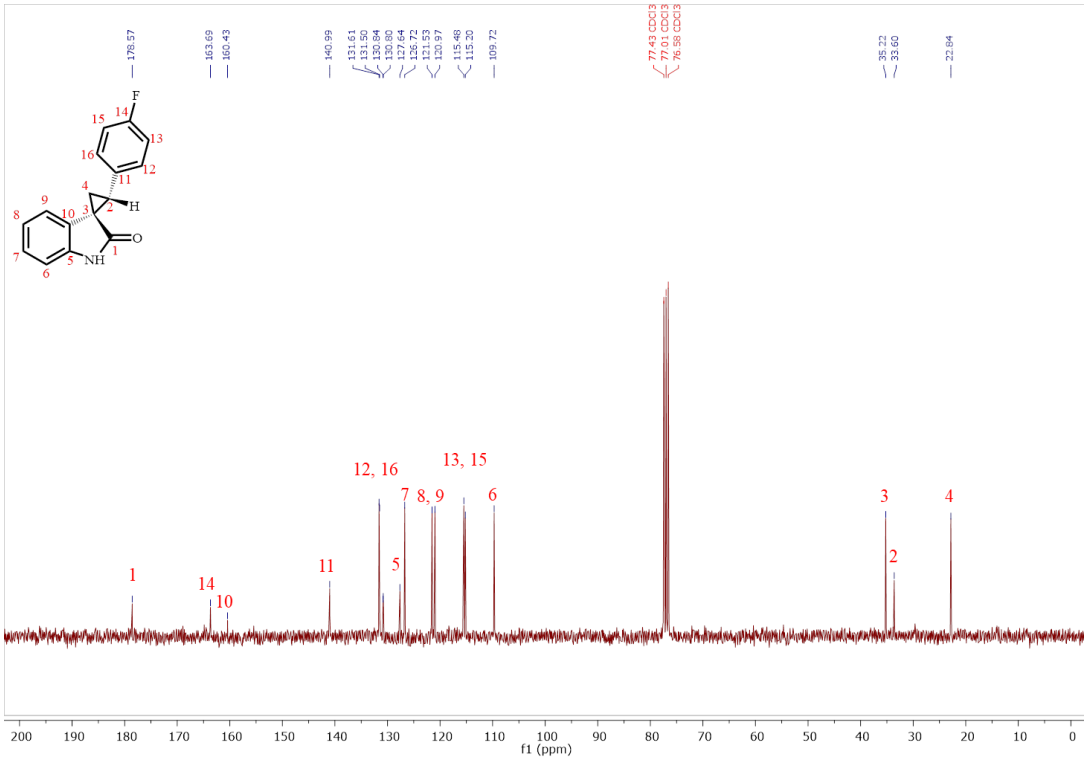


$^{13}$C NMR spectrum of 2-(4-fluorophenyl)spiro[cyclopropane-1,3'-indolin]-2'-one

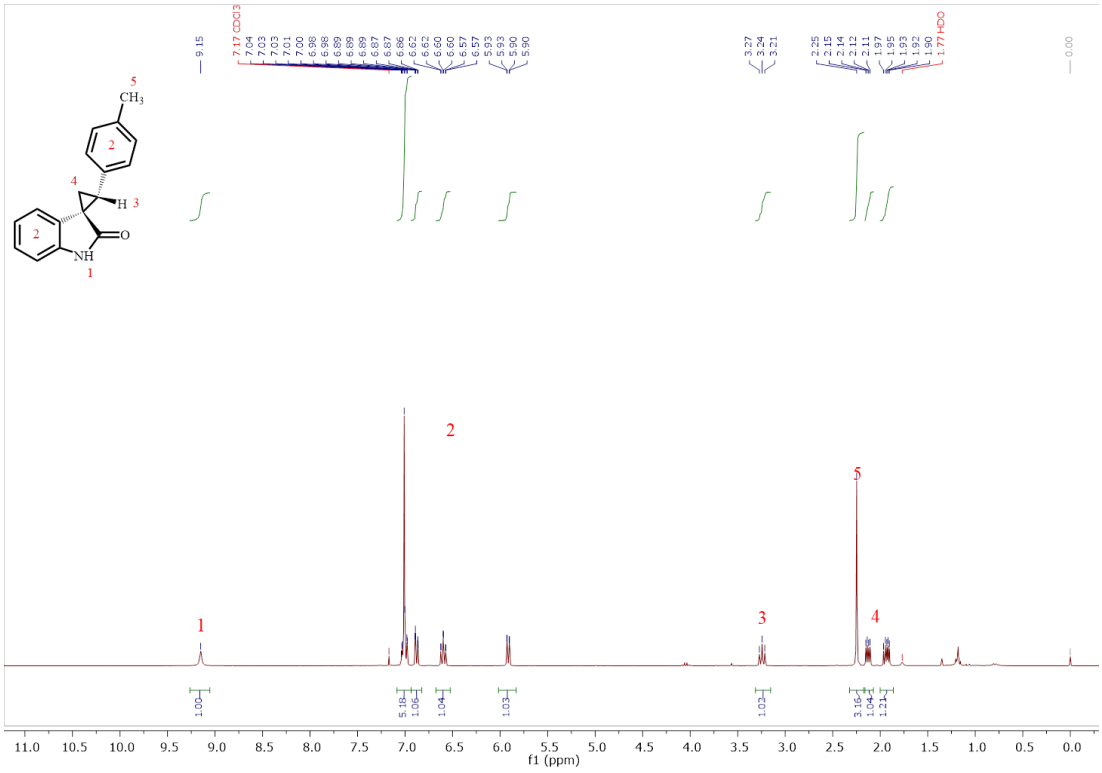


$^{1}$H NMR spectrum of 2-(p-tolyl)spiro[cyclopropane-1,3'-indolin]-2'-one

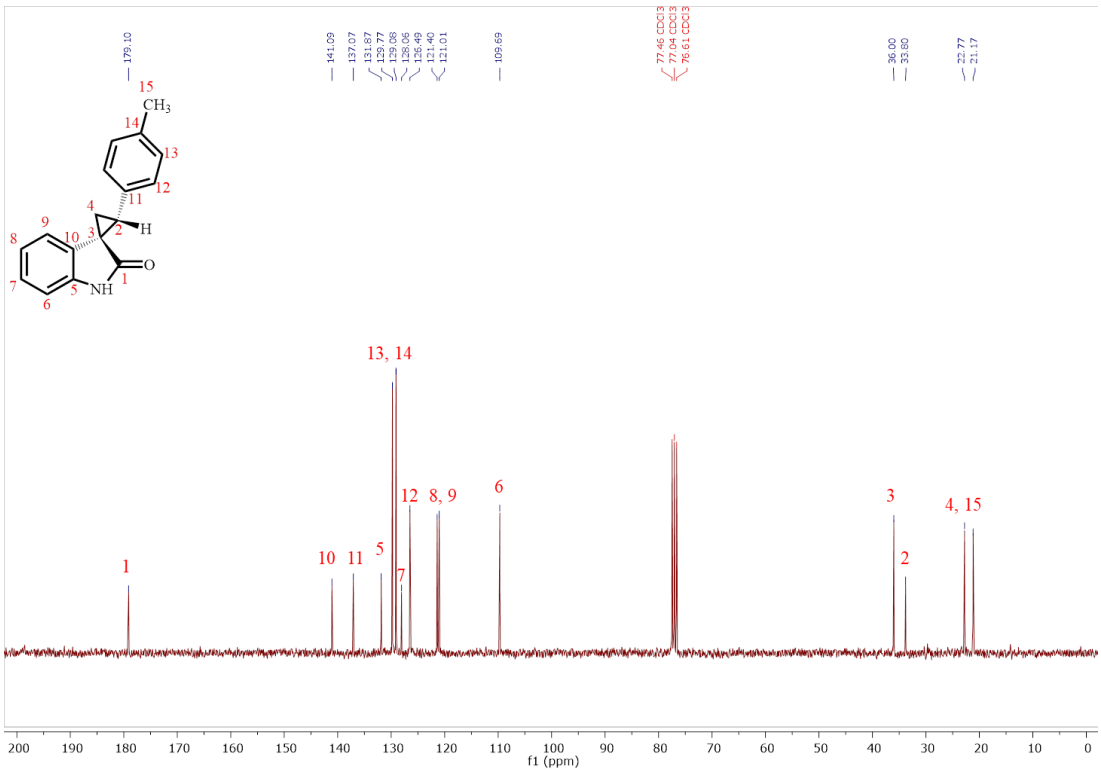


$^{13}$C NMR spectrum of 2-(p-tolyl)spiro[cyclopropane-1,3'-indolin]-2'-one

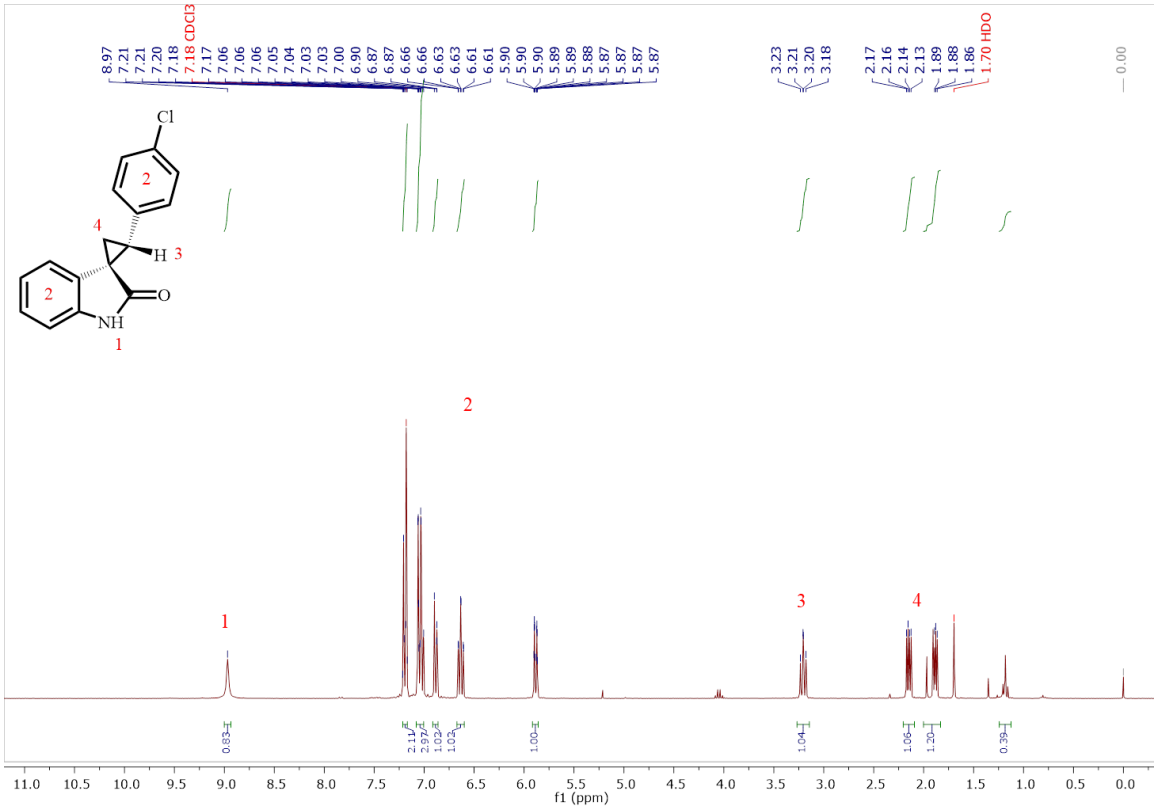


$^{1}$H NMR spectrum of 2-(4-chlorophenyl)spiro[cyclopropane-1,3'-indolin]-2'-one

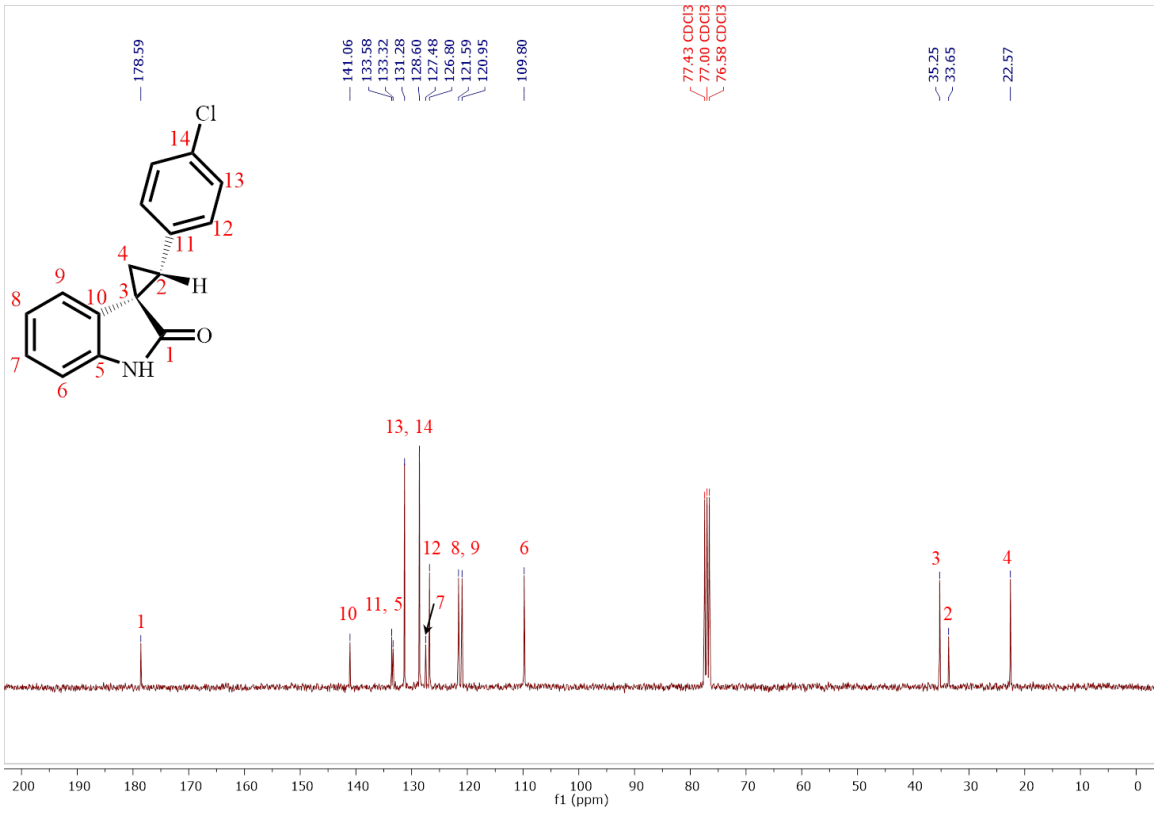


$^{13}$C NMR spectrum of 2-(4-chlorophenyl)spiro[cyclopropane-1,3'-indolin]-2'-one

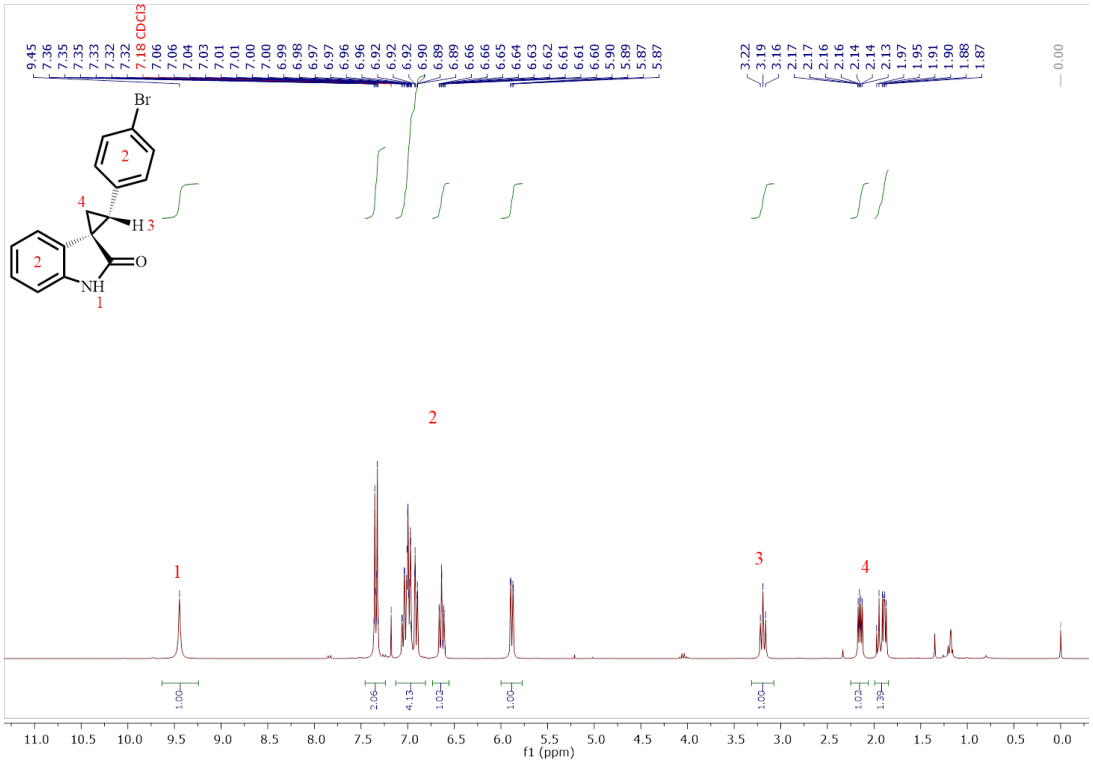


$^{1}$H NMR spectrum of 2-(4-bromophenyl)spiro[cyclopropane-1,3'-indolin]-2'-one

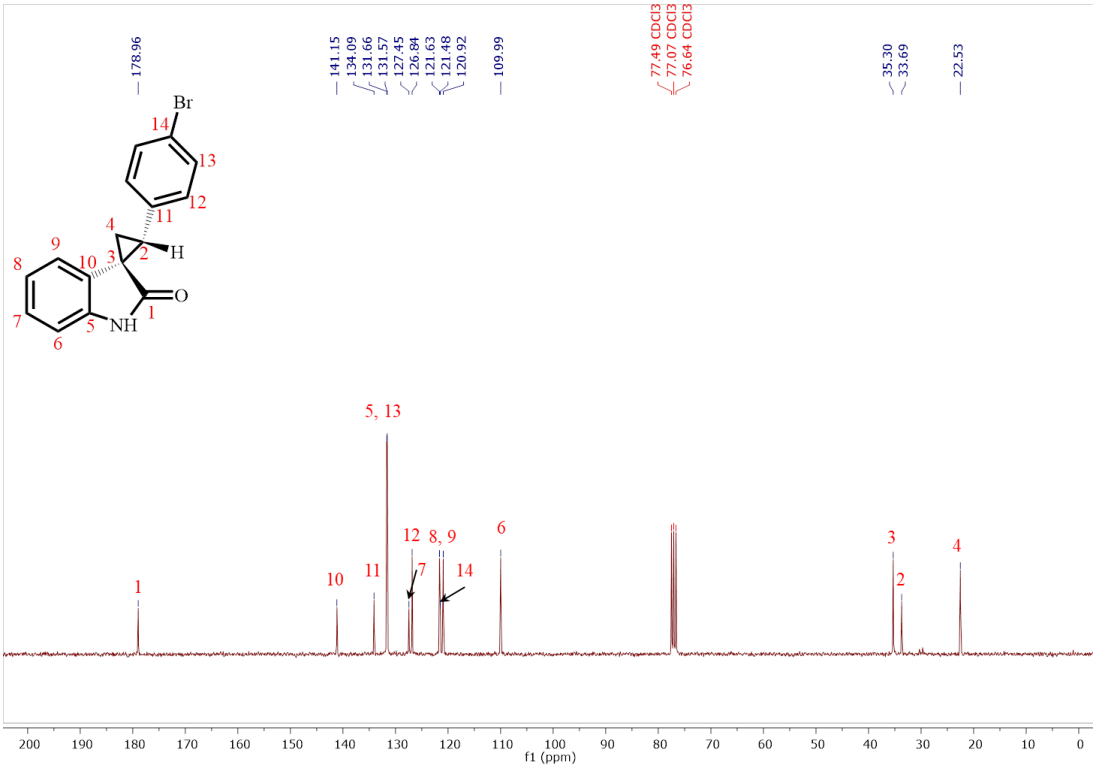


$^{1}$H NMR spectrum of 2-(4-bromophenyl)spiro[cyclopropane-1,3'-indolin]-2'-one

1. Nickerl, G.; Stoeck, U.; Burkhardt, U.; Senkovska, I.; Kaskel, S., A catalytically active porous coordination polymer based on a dinuclear rhodium paddle-wheel unit. *Journal of Materials Chemistry A* **2014,** *2*, 144-148.

2. Li, Z., L. Rösler, K. Herr, M. Brodrecht, H. Breitzke, K. Hofmann, H.-H. Limbach, T. Gutmann, and G. Buntkowsky, Dirhodium Coordination Polymers for Asymmetric Cyclopropanation of Diazooxindoles with Olefins: Synthesis and Spectroscopic Analysis. ChemPlusChem, 2020, 85, 1737-1746.

3. Liu, J.; Xu, Y.; Groszewicz, P. B.; Brodrecht, M.; Fasel, C.; Hofmann, K.; Tan, X.; Gutmann, T.; Buntkowsky, G., Novel dirhodium coordination polymers: the impact of side chains on cyclopropanation. Catal. Sci. Tech. 2018, 8, 5190-5200.

4. Awata, A. and T. Arai, Catalytic asymmetric cyclopropanation with diazooxindole. Synlett, 2013, 24, 29-32.